Available online at www.sciencedirect.com
ScienceDirect
Geochimica et Cosmochimica Acta 75 (2011) 3815–3838
Geochimica et Cosmochimica Acta
www.elsevier.com/locate/gca

Post-collisional granitoids from the Dabie orogen: New evidence for partial melting of a thickened continental crust

Yongsheng He [a,b,*], Shuguang Li [a,*], Jochen Hoefs [b], Fang Huang [a,c], Sheng-Ao Liu [a], Zhenhui Hou [a]

[a] CAS Key Laboratory of Crust-Mantle Materials and Environments, School of Earth and Space Sciences, University of Science and Technology of China, Hefei, 230026 Anhui, China
[b] Department of Geosciences, University of Göttingen, Goldschmidtstr. 1, Göttingen 37077, Germany
[c] Institute of Geochemistry and Petrology, ETH Zurich, 8092 Zurich, Switzerland

Received 25 June 2010; accepted in revised form 11 April 2011; available online 20 April 2011

Abstract

The geological implications of granitoid magmas with high Sr/Y and La/Yb are debated because these signatures can be produced by multiple processes. This study presents comprehensive major and trace element compositions and zircon SHRIMP U–Pb age data of 81 early Cretaceous granitoids and 4 mafic enclaves from the Dabie orogen to investigate partial melting of the thickened lower continental crust (LCC). On the basis of Sr/Y ratios, granitoids can be grouped into two magma series: (i) high Sr/Y granitoids (HSG) and (ii) normal granitoids with low Sr/Y. Relative to normal granitoids, HSG display the following distinct chemical features: (1) at given SiO_2 and CaO contents, the HSG have significantly higher Sr than normal granitoids, defining two different trends in Sr versus SiO_2, CaO diagrams; (2) highly depleted heavy rare earth element (REE) relative to middle and light REE with $(Dy/Yb)_N$ and $(La/Yb)_N$ up to 3.2 and 151, respectively; (3) variable and higher Nb/Ta; and (4) positive correlations among Sr/Y, $(Dy/Yb)_N$, $(La/Yb)_N$, and Nb/Ta.

High Sr/Y, $(La/Yb)_N$, $(Dy/Yb)_N$, and Sr/CaO of HSG do not correlate with major elements (e.g., SiO_2). Large variations in these ratios at a given SiO_2 content indicate that these features do not reflect magma mixing or fractionation. HSG have higher Sr at a given CaO content and larger variation of $(Dy/Yb)_N$ than old crustal rocks (including exposed basement, global mafic LCC xenoliths, high Sr/Y TTG suites, and adakites in modern arcs). This precludes inheritance of the HSG chemical features from these source rocks. Instead, the chemical features of the HSG are best explained by partial melting of the thickened LCC with garnet-dominant, plagioclase-poor, and rutile-present residual lithologies. The coupled chemical features of the HSG are not observed in post-collisional granitoids younger than ca.130 Ma, indicating removal of the eclogitic source and/or residuum of HSG underneath the orogen. These characteristic chemical relationships in the Dabie HSG may be applied to distinguish partial melts of thickened LCC from high Sr/Y intermediate-felsic magmatic rocks which do not show clear indications for melting depth.

1. INTRODUCTION

Granitoid magmas have been widely used as a natural probe to trace the processes of crustal evolution (e.g., Martin et al., 2005; Mo et al., 2007; Wang et al., 2007a). Experimental studies indicate that partial melts from various depths of the continental crust will have distinct geochemical features because the major residual phases change with pressure (e.g., Rapp and Watson, 1995). For example, when

* Corresponding authors at: CAS Key Laboratory of Crust-Mantle Materials and Environments, School of Earth and Space Sciences, University of Science and Technology of China, Hefei, 230026 Anhui, China. Tel.: +86 551 3607647.
E-mail addresses: heys@mail.ustc.edu.cn (Y. He), lsg@ustc.edu.cn (S. Li).

0016-7037/$ - see front matter © 2011 Elsevier Ltd. All rights reserved.
doi:10.1016/j.gca.2011.04.011

a vapor-absent basalt is partially melted, garnet becomes stable at depths greater than ca. 40 km (1.2 GPa) and plagioclase becomes unstable at depths greater than ca. 50 km (1.5 GPa) (e.g., Sen and Dunn, 1994; Rapp, 1995; Rapp and Watson, 1995). Because the heavy rare earth elements (HREE) and Sr are highly compatible in garnet and plagioclase, respectively, partial melting of mafic rocks with garnet dominant and plagioclase poor (or absent) residual phases can produce granitic (sensu lato) melt with high Sr contents, low Y and Yb contents, and high Sr/Y and La/Yb ratios (e.g., Defant and Drummond, 1990; Atherton and Petford, 1993; Rapp, 1995; Rapp and Watson, 1995). These chemically distinct magmas (e.g., $Sr/Y > 40$ and $Y < 18$ ppm) were first termed as adakites which were originally interpreted to represent melts of descending slabs (Defant and Drummond, 1990). Later adakite-like melts also have been widely reported in continental settings, generally being interpreted as partial melts of the thickened or delaminated eclogitic lower continental crust (LCC) (e.g., Atherton and Petford, 1993; Zhang et al., 2001; Xu et al., 2002, 2007; Chung et al., 2003; Gao et al., 2004; Wang et al., 2004a,b, 2005, 2006, 2007a,b; Liu et al., 2010a). Archean TTG (tonalite–trondhjemite–granodiorite) suites generally also have high Sr/Y ratios (e.g., Martin, 1999; Condie, 2005; Martin et al., 2005). Granitoid magmas of this type may thus be crucial indicators for (i) the presence of a thickened continental crust (e.g., Atherton and Petford, 1993; Wang et al., 2007a), (ii) a change of crustal thickness (e.g., Wang et al., 2007a; Xu et al., 2007), (iii) the recycling of eclogitic crust (e.g., Defant and Drummond, 1990; Kay and Kay, 1993; Martin et al., 2005; Huang et al., 2008), and (iv) the origin of early continental crust (e.g., Martin, 1999; Condie, 2005; Martin et al., 2005).

However, the geological implications of granitoid magmas with high Sr/Y and La/Yb are highly debated because these signatures can be produced by multiple processes. Several recent studies suggest that high Sr/Y and La/Yb ratios can be produced by processes other than partial melting of mafic crust at depths >50 km, e.g., assimilation and fractional crystallization (e.g., Macpherson et al., 2006; Richards and Kerrich, 2007; Li et al., 2009), magma mixing (e.g., Chen et al., 2004; Guo et al., 2007), melting of granulites (e.g., Jiang et al., 2007), and melting of high Sr/Y and La/Yb sources at low pressure (e.g., Kamei et al., 2009; Moyen, 2009; Zhang et al., 2009). Therefore, a better understanding of the chemical differences between partial melts from mafic crust at depths >50 km and those from other crustal processes is necessary.

The Dabie orogen in central China is a part of the Triassic collisional zone between the South China and the North China Block (Li et al., 1993, 2000). The post-collisional granitoids in the orogen are characterized by the occurrence of high Sr/Y granitoids (HSG) at >130 Ma and mafic rocks and normal (generally low Sr/Y) granitoids at <130 Ma (Ma et al., 2003; Zhao et al., 2005; Wang et al., 2007a; Xu et al., 2007). This compositional transition has been interpreted by partial melting of thick versus thin crust during the mountain root removal process in the orogen (Ma et al., 2003; Wang et al., 2007a; Xu et al., 2007). However, as discussed above, HSG may be produced by multiple processes, and thus the geological meaning of the compositional transition is ambiguous. More geochemical studies are needed to identify high Sr/Y granitoids in the Dabie orogen and to constrain the depth of partial melting in the thickened lower continental crust.

Here, we report major and trace element data for 81 granitoids and 4 melanocratic enclaves from the Dabie orogen together with zircon U–Pb age data. The objectives of this contribution are (1) to provide a systematic geochemical study of the post-collisional granitoids in the Dabie orogen, (2) to present criteria for the identification of partial melts of thickened crust by comparing high Sr/Y granitoids with other granitoids, and (3) to understand the petrogenetic relationships between high Sr/Y and normal granitoids, and thereby constraining the mountain root removal process of the Dabie orogen.

2. GEOLOGICAL SETTING

The geologic background of the Dabie orogen has been extensively discussed in the literature (e.g., Li et al., 1993, 2000, 2001; Hacker et al., 1998; Liu et al., 2007b). Briefly, the Dabie orogen is a Triassic collisional zone between the South China Block (SCB) and the North China Block (NCB) (Fig. 1). The orogen can be divided into four units from north to south: the North Huaiyang zone (NHZ), the North Dabie zone (NDB), the South Dabie zone (SDB), and the Susong high pressure metamorphic zone (HPZ) (Li et al., 2001). Exposed coesite and diamond bearing ultrahigh pressure metamorphic (UHPM) rocks indicate that the continental crust of SCB was subducted to depths greater than 100 km in the early Triassic (e.g., Okay et al., 1989; Wang et al., 1989; Xu et al., 1992; Ye et al., 2000). Although a very thick continental crust was produced by the continent–continent collision, seismologic investigations show that the current Dabie orogen has a normal crust thickness averaging ~35 km without a lithospheric keel (Gao et al., 1998; Yuan et al., 2003). This indicates that the mountain root, consisting of the lithospheric keel and thickened mafic lower crust, may have been foundered and consequently recycled into the underlying uppermost mantle.

Early Cretaceous post-collisional igneous rocks are widely distributed in the Dabie orogen (Fig. 1) (e.g., Li et al., 1998a,b; Ma et al., 1998, 2003; Jahn et al., 1999; Chen et al., 2002; Zhang et al., 2002; Fan et al., 2004; Xie et al., 2004, 2006; Zhao et al., 2005, 2007a,c; Huang et al., 2007, 2008; Wang et al., 2007a; Xu et al., 2007). They mainly consist of intermediate to felsic granitoid plutons, with a few mafic intrusions. Granitoids have intrusive ages spanning from 143 to 117 Ma (Wang et al., 2007a and reference therein). The early granitoid plutons (143–130 Ma) generally display high Sr/Y and La/Yb features (Ma et al., 2003; Wang et al., 2007a; Xu et al., 2007), whereas the later granitoid plutons younger than 130 Ma do not have high Sr/Y and La/Yb ratios (Wang et al., 2007a; Xu et al., 2007). Mafic to ultramafic intrusions were emplaced from 130 to 123 Ma (Hacker et al., 1998; Li et al., 1999; Wang and Deng, 2002; Zhao et al., 2005). The older granitoids are weakly deformed with banded textures and are intruded by mafic or

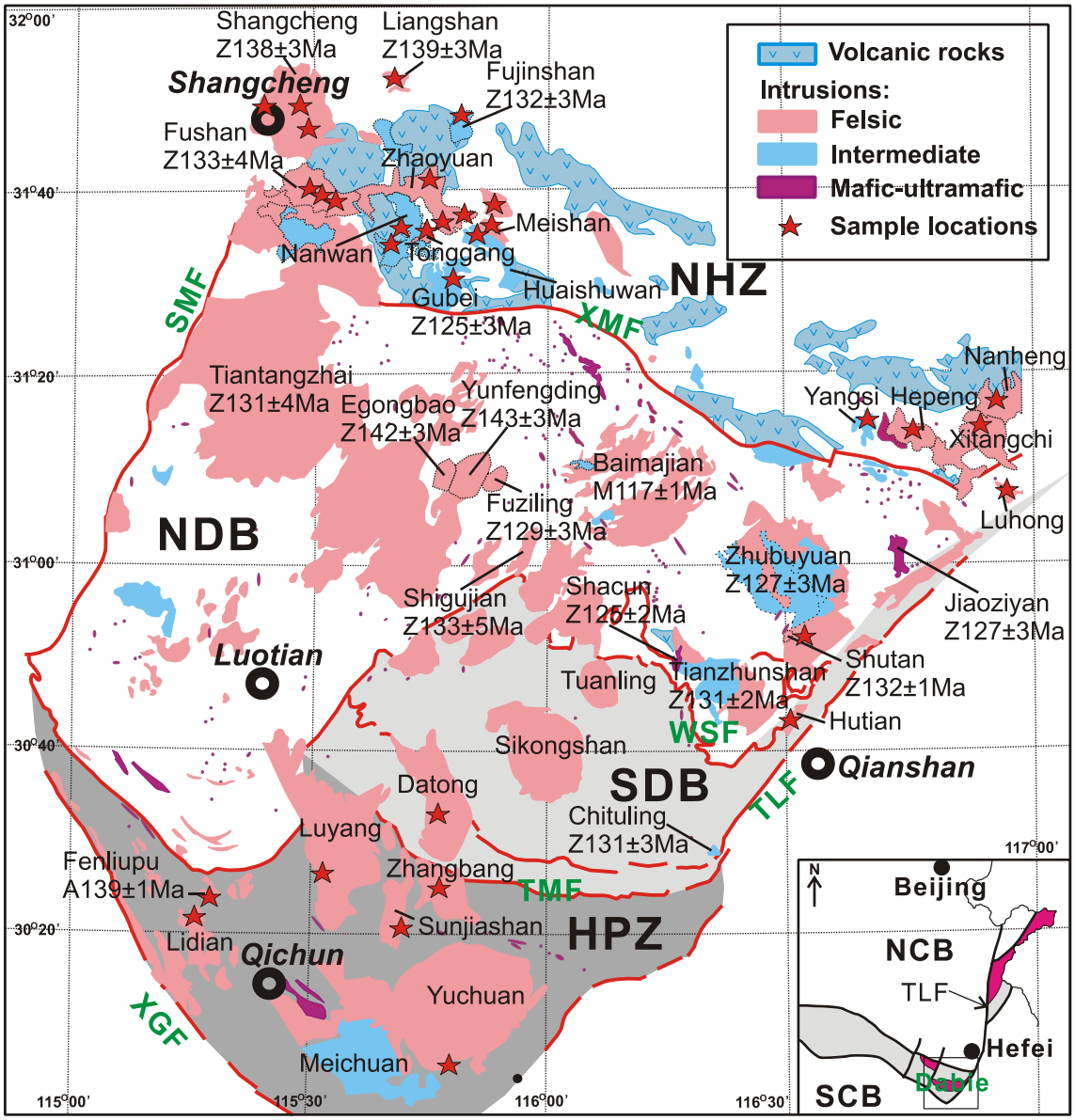

Fig. 1. Generalized geological map of the Dabie orogen. NHZ, NDB, SDB, and HPZ represent the North Huaiyang Zone, the North Dabie Zone, the South Dabie Zone, and the Susong High Pressure Metamorphic Zone, respectively. XMF, SMF, WSF, TMF, XGF and TLF are abbreviations of the Xiaotian–Mozitan Fault, the Shangcheng–Macheng Fault, the Wuhe–Shuihou Fault, the Taihu–Mamiao Fault, the Xiangfan–Guangji Fault and the Tancheng–Lujiang Fault, respectively. Age data for plutons are from Ma et al. (2003), Zhao et al. (2005, 2007a,c), Xie et al. (2006), Wang et al. (2007a), Xu et al. (2007), Huang et al. (2008), and this study. Zircon U–Pb ages are characterized by Z, and amphibole Ar–Ar ages by A.

granitic dikes, whereas the younger granitoids exhibit extensively igneous textures without deformation (e.g., Ma et al., 2003; Wang et al., 2007a; Xu et al., 2007). One high-Mg adakitic pluton (131 Ma) has been reported in the SDZ close to the Tan-Lu fault, suggesting local delamination of the eclogitic lower crust (Huang et al., 2008).

Notably, dark (mafic to intermediate) enclaves have been found both in some HSG and normal granitoids (Table A1; Chen et al., 2002; Zhang et al., 2010). The enclaves show lobate to spherical contacts with the enclosing granitoids, indicating that these rock units coexisted during contemporaneous magmatism. Field outcrops and thin sections indicate that melanocratic enclaves consist of plagioclase, hornblende, biotite, ± pyroxene, ± K-feldspar, ± quartz, and accessory titanite, apatite, zircon with minor amounts of opaque minerals.

Because granitoids from the NDZ have been extensively studied (see Zhao and Zheng (2009) for a recent review), this study sampled 81 granitoids and 4 melanocratic enclaves with most of them from NHZ, SDB, and HPZ. Sample locations are shown in Fig. 1. Detailed petrographic descriptions are given in the Appendix A.

3. ANALYTICAL METHODS

Fresh samples were crushed in steel jaw crushers and then powdered in an agate mill to grain sizes <200 mesh at the Department of Geosciences, University of Göttingen. Major and trace elements were analyzed in Göttingen using a PANalytical AXIOS advanced sequential X-ray spectrometer. The long term analytical precision is better than 1–2% for major elements and in the range of 2–5% at the level of 20–30 ppm for trace elements. Duplicate measurements of two in-house standards (basalt BB and granodiorite GD, 14 and 35 times, respectively) and one international standard (JR-1, 4 times) display the long term precision (Appendix C, Table C1). Loss of ignition (LOI) was determined by gravimetric methods. In order to get accurate data for elements with low contents (e.g., HREE) and avoid sample dissolution problems, some trace elements (Appendix B) were also analyzed by LA-ICPMS on lithium borate glasses using a GeolasPro ArF (193 nm) excimer laser sampling system coupled with a Perkin Elmer Elan DRCII at the University of Science and Technology of China, Hefei. USGS reference standards, GSP-2, BHVO2, and W-2a, were repeatedly measured 10, 5, and 4 times, respectively. Sample 07LS-1, a typical HSG with almost lowest Y and HREE, was measured 5 times. Duplicate analyses suggest that for most elements, precision are better than 5% and accuracies better than 10%. The reported values are normalized by W-2a against the recommended value (GeoRem, http://georem.mpch-mainz.gwdg.de/). For comparison, some Liangshan and Zhangbang samples (Appendix B, Table B3) were also analyzed at the Guangzhou Institute of Geochemistry, Chinese Academy of Sciences by solution ICPMS method using Parr bombs as described by (Liu et al., 2007a). Analytical precision for most elements is better than 3%. Comparison of the data by the two methods and the recommended values for standards indicates that Nb/Ta and the high $(Dy/Yb)_N$ are reliable for the LA-ICPMS data (Appendix B). LA-ICPMS data will be preferentially used in the following discussion because of its advantage of measuring HREE and HFSE.

For the determination of U–Pb ages, zircon crystals were separated using conventional heavy liquid and magnetic separation techniques followed by handpicking under binocular microscope. About 200 zircon grains of four samples from the North Huaiyang zone and some grains of the zircon U–Pb standard TEMORA 1 (417 Ma, Black et al., 2003) were mounted together, and polished until all zircon grains were well exposed. Internal zoning patterns of the crystals were observed using CL images at the Institute of Mineral Resources, Chinese Academy of Geological Sciences (GAGS). Zircon U–Pb ages were determined using a SHRIMP II at the Beijing SHRIMP center, GAGS, following the method described by Compston et al. (1992), Williams (1998) and Liu et al. (2006). The TEMORA 1 standard data was used to calibrate $^{206}Pb/^{238}U$ ages. Absolute U, Th and Pb concentrations were estimated with a separately mounted fragment of RSES reference zircon SL13 (572 Ma, U ≈ 238 ppm) (Williams, 1998). Common Pb was corrected using the measured ^{204}Pb. The PRAWN data reduction software (Williams, 1998) was used for data processing for each spot, and ages were calculated using the constants recommended by Steiger and Jäger (1977). Weighted zircon U–Pb ages were calculated using the ISOPLOT program (Ludwig, 2001).

4. RESULTS

4.1. Major and trace elements

Major and trace elements for 85 samples are listed in Table 1 and Appendix C, Table C1. Based on Sr/Y and Y contents, the Dabie granitoid plutons are generally divided into two groups: (i) high Sr/Y granitoids (HSG, with Sr/Y > 40 and Y < 18 ppm) and (ii) 'normal granitoids' (Fig. 2). With a few exceptions, normal granitoids have low Sr contents, Sr/Y, and high Y relative to the HSG (Fig. 2). Some samples (for example, Zhubuyuan) (Chen et al., 2002; Zhang et al., 2002; Zhao et al., 2004), do not follow this classification. In these cases, the pluton is classified according to the majority of the samples.

All Dabie HSG reported in this study have low MgO, Cr and Ni contents with Mg# <50 (Appendix C, Table C1), comparable to (i) experimental melts from pristine basaltic sources (Rapp et al., 1991, 1999; Sen and Dunn, 1994; Rapp, 1995; Rapp and Watson, 1995), to (ii) partial melts of thickened continental crust (Atherton and Petford, 1993), and (iii) to the majority of Archean high Sr/Y TTG suites (Condie, 2005; Smithies, 2000). By contrast, adakites in modern arcs and those derived from delaminated lower continental crust generally have Mg# >50 (e.g., Defant and Drummond, 1990; Huang et al., 2008). High-Mg HSG from Dabie described in the literature are not included here because they seem to have experienced melt/mantle interaction (Huang et al., 2008).

HSG and normal granitoids are similar in most major element Harker diagrams (e.g., Fig. 3A). However, the HSG have major elemental compositions with a much smaller range than normal granitoids. In a diagram of total alkali versus SiO_2, normal granitoids are mainly in the monzonite, quartz monzonite, and granitoid fields with a large variation in SiO_2 from 54.3 to 78.7 wt% (Fig. 3A). They are metaluminous to weakly peraluminous (A/CNK from 0.70 to 1.13) (Fig. 3B), which is typical for I-type granitoids (Chappell and White, 1992). By contrast, most HSG have SiO_2 from 64.0 to 75.0 wt% and A/CNK from 0.90 to 1.10. The HSG have slightly higher Na_2O and Na_2O/K_2O than normal granitoids at a given SiO_2 (Fig. 3C and D). This feature is also found in adakites, being relatively enriched in Na_2O compared to relevant arc andesites to rhyolites (Defant and Drummond, 1990).

In REE diagrams (Fig. 4A), normal granitoids generally have LREE-enriched patterns with no obvious negative Eu anomalies. A few normal granitoids with high SiO_2 (e.g., 06ZY-3, a late dike; 06HSW-2) show strong negative Eu anomalies and/or down-concave REE patterns. Except sample 07LD-4 and samples from Fuziling (Wang et al., 2007a), the HSG also have LREE-enriched REE patterns and show no obvious Eu anomalies (Fig. 4C). The HSG generally have low HREE contents relative to normal granitoids (Fig. 4C). Furthermore, the HSG generally have

Table 1
Major and trace element concentrations of representative samples. (1) HSG, NG, and Enc represent high Sr/Y granitoids, normal (low Sr/Y) granitoids, and enclaves. (2) Major elements are measured by XRF and are from Table C1 in Appendix C. Major elements of samples ($n = 7$) marked by * have been published previously in Liu et al. (2010b). Trace elements are measured by LA-ICPMS on XRF glasses. (3) Four samples marked by ** yield internal precisions lower than the rest, but are <15% for most elements (For details see the Appendix B, Fig.B2).

Intrusion	Liangshan	Liangshan	Liangshan	Liangshan	Liangshan	Shangcheng	Shangcheng	Shangcheng	Shangcheng	Shangcheng
Sample	07LS-1	07LS-2	06LS-2	07LS-3**	07LS-5	06FJ-1	06FJ-2	06FJ-3**	07FJ-1**	07FJ-2*
Classify	HSG	HSG	HSG	HSG	HSG	HSG	HSG	HSG	HSG	HSG
SiO_2	69.26	69.06	70.61	69.07	67.78	71.95	69.41	69.32	68.16	68.50
TiO_2	0.295	0.273	0.267	0.301	0.290	0.278	0.377	0.407	0.507	0.451
Al_2O_3	15.55	15.50	15.34	15.47	15.03	14.20	15.33	15.18	15.70	15.27
Fe_2O_3t	1.57	1.61	1.41	1.52	1.68	1.64	2.11	2.27	2.66	2.53
MnO	0.024	0.025	0.017	0.019	0.029	0.030	0.030	0.034	0.042	0.041
MgO	0.41	0.46	0.42	0.29	0.59	0.69	0.65	0.67	0.82	0.80
CaO	1.15	1.39	0.85	1.33	2.23	1.67	1.84	1.97	2.05	2.07
Na_2O	4.74	4.97	4.75	4.69	4.24	4.26	4.53	4.64	4.71	4.68
K_2O	4.11	4.09	4.16	4.15	3.80	3.80	4.31	3.89	4.27	4.07
P_2O_5	0.098	0.095	0.086	0.103	0.100	0.088	0.136	0.143	0.164	0.176
LOI	1.78	1.81		1.90	3.75		0.39			
Sum	98.99	99.28	97.91	98.84	99.52	98.61	99.11	98.52	99.08	98.59
Mg#	34	36	37	28	41	46	38	37	38	39
Rb	82	80	82	84	79	91	108	94	91	102
Sr	761	841	951	1037	657	832	897	864	1016	1047
Y	3.8	3.7	4.1	4.2	3.9	4.3	6.9	7.4	9.7	8.5
Zr	167	175	170	179	170	131	181	186	211	203
Nb	4.5	4.5	4.5	4.6	4.6	4.5	7.4	7.5	9.6	8.8
Cs	2.7	1.7	2.4	2.7	2.4	1.1	1.5	1.1	0.83	1.5
Ba	2292	2198	2336	2538	2103	1851	2172	1785	2624	2055
La	41	42	46	45	42	26	45	49	57	53
Ce	75	78	73	85	79	49	84	89	106	97
Pr	8.2	8.5	9.0	9.4	8.5	5.3	9.0	9.6	12	10
Nd	29	30	32	34	30	18	32	34	42	37
Sm	4.5	4.5	4.7	5.4	4.6	2.8	4.8	5.3	6.1	5.7
Eu	1.1	1.2	1.3	1.4	1.2	0.81	1.3	1.3	1.5	1.4
Gd	2.5	2.6	2.7	2.9	2.7	1.8	3.0	3.1	3.8	3.4
Tb	0.24	0.25	0.28	0.23	0.25	0.19	0.35	0.35	0.44	0.39
Dy	0.88	0.91	0.96	1.04	0.94	0.84	1.5	1.5	2.0	1.7
Ho	0.13	0.13	0.14	0.14	0.13	0.14	0.24	0.26	0.32	0.28
Er	0.27	0.26	0.32	0.33	0.29	0.34	0.59	0.63	0.80	0.70
Tm	0.034	0.037	0.042	0.040	0.035	0.051	0.079	0.085	0.11	0.098
Yb	0.20	0.20	0.22	0.25	0.20	0.30	0.49	0.51	0.60	0.59
Lu	0.028	0.031	0.034	0.032	0.029	0.051	0.074	0.076	0.094	0.087
Hf	4.6	4.8	4.5	5.5	4.8	3.2	4.8	5.0	5.3	5.1
Ta	0.24	0.24	0.25	0.27	0.24	0.26	0.45	0.50	0.57	0.53
Pb	27	17	24	28	35	20	22	21	21	21
Th	8.8	9.1	8.8	10	9.1	5.7	9.6	12	12	10
U	1.2	1.5	1.2	1.6	1.6	1.1	1.6	1.7	1.2	1.4
$(La/Yb)_N$	147	151	150	129	151	62	66	69	68	64
$(Dy/Yb)_N$	2.9	3.0	2.9	2.8	3.1	1.9	2.0	2.0	2.2	1.9
$(Gd/Yb)_N$	10	11	10	9.6	11	5.0	5.1	5.0	5.2	4.8
Sr/Y	200	227	231	247	168	193	130	117	105	123

(*continued on next page*)

Table 1 (*continued*)

Intrusion	Shangcheng	Shangcheng	Shangcheng	Shangcheng	Shangcheng	Shangcheng	Datong	Datong	Fenliupu	Fenliupu
Sample	07FJ-4	07FJ-5	07FJ-6*	07FJ-7	07FJ-8	07FJ-9	07DT-2	07DT-3*	07FLP-1	07FLP-2
Classify	HSG	HSG	HSG	HSG	HSG	HSG	HSG	HSG	HSG	HSG
SiO_2	68.35	68.45	67.91	69.28	69.60	69.48	64.77	66.22	69.49	69.80
TiO_2	0.451	0.443	0.478	0.363	0.426	0.412	0.729	0.704	0.309	0.334
Al_2O_3	14.63	14.92	14.92	15.24	15.08	15.25	16.28	15.16	15.51	15.17
Fe_2O_3t	3.15	3.17	3.38	2.48	2.33	2.28	3.60	3.80	2.03	2.14
MnO	0.074	0.068	0.071	0.054	0.036	0.035	0.054	0.060	0.046	0.049
MgO	1.34	1.32	1.44	1.02	0.69	0.67	1.35	1.37	0.61	0.63
CaO	2.67	2.88	3.03	2.58	1.95	1.95	2.64	2.32	2.01	1.97
Na_2O	3.88	4.00	4.08	4.08	4.56	4.74	4.48	4.15	4.67	4.55
K_2O	3.89	3.64	3.50	4.10	3.99	4.00	4.38	4.29	3.90	3.89
P_2O_5	0.166	0.169	0.184	0.135	0.155	0.148	0.314	0.300	0.144	0.157
LOI										
Sum	98.60	99.06	98.99	99.33	98.82	98.97	98.60	98.37	98.72	98.69
Mg#	46	45	46	45	37	37	43	42	38	37
Rb	110	96	99	118	98	96	88	93	101	103
Sr	645	669	685	679	855	859	1353	1138	953	909
Y	11	12	13	8.9	7.9	7.4	13	15	7.7	8.5
Zr	152	151	166	123	194	189	274	274	156	164
Nb	9.7	9.0	11	7.7	8.1	7.7	16	19	11	12
Cs	2.1	1.7	2.0	2.1	1.0	1.2	1.2	1.2	1.8	1.9
Ba	1230	1186	1173	1609	1854	1909	3825	3597	1934	1896
La	43	36	41	29	52	47	70	68	28	31
Ce	73	66	75	52	94	88	137	133	52	56
Pr	7.4	7.2	8.1	5.5	10	9.3	15	15	5.5	6.0
Nd	26	25	29	19	36	33	53	53	20	21
Sm	4.0	4.2	4.8	3.1	5.4	4.9	8.3	8.3	3.2	3.5
Eu	1.1	1.1	1.3	0.85	1.3	1.2	2.2	2.1	0.91	0.91
Gd	2.9	3.0	3.4	2.2	3.3	3.0	4.9	5.2	2.2	2.3
Tb	0.39	0.38	0.44	0.29	0.38	0.35	0.57	0.60	0.28	0.30
Dy	2.0	2.0	2.2	1.5	1.6	1.5	2.7	3.1	1.4	1.5
Ho	0.37	0.39	0.42	0.29	0.27	0.24	0.44	0.50	0.25	0.27
Er	1.1	1.1	1.2	0.81	0.64	0.56	1.2	1.4	0.67	0.71
Tm	0.15	0.16	0.18	0.13	0.086	0.080	0.16	0.20	0.097	0.11
Yb	1.0	0.97	1.1	0.81	0.53	0.49	0.93	1.2	0.63	0.65
Lu	0.17	0.16	0.19	0.13	0.081	0.071	0.13	0.17	0.092	0.10
Hf	4.1	4.0	4.3	3.5	5.0	4.8	6.2	6.3	4.4	4.6
Ta	0.66	0.62	0.71	0.53	0.52	0.47	0.81	1.3	0.86	0.95
Pb	28	22	24	25	22	21	25	26	30	31
Th	15	11	13	12	11	11	8.4	8.1	5.8	6.2
U	3.9	2.8	4.1	2.3	1.6	1.7	0.95	1.1	2.2	2.1
$(La/Yb)_N$	31	27	27	26	70	69	54	41	32	34
$(Dy/Yb)_N$	1.3	1.4	1.3	1.2	2.0	2.0	1.9	1.7	1.5	1.5
$(Gd/Yb)_N$	2.4	2.6	2.6	2.2	5.2	5.1	4.4	3.6	2.9	2.9
Sr/Y	58	56	53	76	108	116	104	76	124	107

SiO_2	69.40	69.08	68.86	67.59	72.39	67.69	67.78	65.63	65.88	64.56
TiO_2	0.421	0.309	0.371	0.399	0.123	0.536	0.524	0.570	0.551	0.572
Al_2O_3	15.11	15.66	15.79	15.63	15.48	16.11	15.95	16.57	16.34	16.82
Fe_2O_3t	2.37	2.03	2.28	2.62	0.80	2.24	2.30	2.93	2.71	3.10
MnO	0.054	0.048	0.046	0.056	0.024	0.029	0.029	0.034	0.034	0.041
MgO	0.81	0.60	1.08	1.30	0.19	0.90	0.93	1.21	1.09	1.27
CaO	1.94	1.90	2.37	2.46	1.40	2.11	2.15	2.42	2.29	2.66
Na_2O	4.70	4.82	4.71	4.68	5.33	5.03	5.04	5.29	5.04	5.23
K_2O	3.71	3.84	3.82	3.69	3.41	3.91	3.70	3.58	3.98	3.96
P_2O_5	0.156	0.142	0.174	0.209	0.032	0.159	0.155	0.252	0.242	0.269
LOI										
Sum	98.67	98.43	99.50	98.63	99.18	98.71	98.56	98.49	98.16	98.48
Mg#	41	37	49	50	32	45	45	45	45	45
Rb	73	92	71	82	74	73	67	72	80	89
Sr	915	884	1487	1421	1202	1585	1595	1730	1613	1598
Y	6.2	7.2	10.0	11	3.6	7.0	7.6	7.4	7.3	7.1
Zr	229	168	173	174	63.5	218	227	254	241	246
Nb	4.6	9.9	10	13	5.0	8.6	8.9	8.9	8.7	8.4
Cs	0.94	1.7	1.3	2.0	1.0	0.72	0.79	0.81	0.80	0.85
Ba	2012	1659	2416	2231	1446	3915	3698	3602	3910	3501
La	50	30	35	35	4.2	65	69	71	68	68
Ce	86	54	65	64	8.5	119	125	129	123	123
Pr	8.7	5.7	7.2	7.1	0.98	13	14	14	13	13
Nd	30	21	26	27	3.6	46	49	49	48	47
Sm	4.3	3.1	4.3	4.4	0.73	6.8	7.4	7.2	7.0	6.9
Eu	1.1	0.84	1.2	1.2	0.30	1.9	2.0	1.9	2.0	1.9
Gd	2.7	2.0	2.8	3.0	0.88	3.9	4.1	4.0	4.0	3.8
Tb	0.31	0.26	0.36	0.38	0.13	0.41	0.44	0.42	0.41	0.40
Dy	1.3	1.3	1.8	1.9	0.74	1.6	1.7	1.6	1.7	1.6
Ho	0.22	0.23	0.33	0.36	0.13	0.23	0.26	0.24	0.25	0.24
Er	0.53	0.62	0.86	0.97	0.32	0.53	0.57	0.54	0.56	0.55
Tm	0.073	0.10	0.13	0.14	0.048	0.067	0.075	0.072	0.071	0.073
Yb	0.43	0.63	0.82	0.88	0.33	0.36	0.41	0.41	0.41	0.40
Lu	0.070	0.10	0.13	0.14	0.037	0.055	0.054	0.057	0.058	0.060
Hf	5.6	4.5	4.9	5.2	2.3	5.2	5.5	5.6	5.7	5.8
Ta	0.31	0.66	0.72	0.89	0.56	0.51	0.54	0.48	0.51	0.48
Pb	17	32	32	33	41	26	24	23	26	28
Th	17	6.4	8.1	7.8	1.4	7.7	8.1	7.8	7.9	7.8
U	1.8	2.0	1.9	2.2	1.3	1.0	0.88	0.84	0.84	0.88
$(La/Yb)_N$	83	34	31	29	9.1	130	121	124	119	122
$(Dy/Yb)_N$	2.0	1.4	1.5	1.4	1.5	3.0	2.8	2.6	2.8	2.7
$(Gd/Yb)_N$	5.2	2.6	2.8	2.8	2.2	9.0	8.3	8.1	8.1	7.9
Sr/Y	147	123	149	129	334	226	210	234	221	225

(*continued on next page*)

Table 1 (*continued*)

Intrusion	Sujiashan	Xima	Xima	Huaishuwan	Yuchan	Yuchan	Zhaoyuan	Meishan	Tonggang	Tonggang	Zhaoyuan
Sample	07SJS-2	07XM-1	07XM-3	07XT-1	07YC-1	07YC-3	06NW-5	06SF-1	06TG-1	06TG-2	06ZY-2
Classify	NG	NG	NG	NG	NG	NG	NG	NG	NG	NG	NG
SiO_2	74.04	67.37	68.38	73.63	71.76	69.28	66.44	62.29	61.09	60.09	66.17
TiO_2	0.202	0.611	0.398	0.242	0.360	0.306	0.515	0.700	0.679	0.896	0.533
Al_2O_3	13.75	15.14	15.48	12.91	13.96	15.19	15.61	16.12	18.41	17.09	15.30
Fe_2O_3t	1.47	3.57	2.61	1.43	2.19	1.88	3.51	5.03	4.01	6.07	3.98
MnO	0.041	0.056	0.050	0.030	0.032	0.033	0.039	0.099	0.063	0.081	0.074
MgO	0.38	1.13	0.72	0.47	0.57	0.46	1.49	2.23	1.51	1.98	1.63
CaO	1.59	2.52	2.11	1.15	1.58	1.56	2.73	4.15	4.49	4.51	3.07
Na_2O	3.78	3.84	4.09	3.18	3.48	3.67	4.30	3.80	4.95	4.44	3.77
K_2O	4.05	4.52	4.40	4.74	4.78	5.71	2.98	3.47	2.91	3.06	4.31
P_2O_5	0.061	0.223	0.136	0.059	0.106	0.094	0.189	0.217	0.256	0.368	0.192
LOI											
Sum	99.36	98.98	98.37	97.84	98.82	98.18	97.80	98.11	98.37	98.59	99.03
Mg#	34	39	36	40	34	33	46	47	43	39	45
Rb	118	122	130	166	96	112	73.8	105	60	68	131
Sr	254	557	663	162	413	473	709	574	1026	907	581
Y	15	26	16	11	18	19	15	18	17	27	16
Zr	133	348	274	110	227	195	195	173	196	283	214
Nb	14	31	17	14	15	20	11	11	11	16	12
Cs	1.0	0.55	1.3	3.6	0.55	0.51	1.6	3.2	1.4	1.9	2.9
Ba	1048	2259	2188	932	1731	2439	1656	1724	2247	2128	1595
La	31	112	87	43	83	82	51	49	46	64	51
Ce	56	208	156	71	142	149	94	87	89	132	92
Pr	5.7	21	15	6.8	14	15	9.9	9.2	10	15	9.4
Nd	19	67	48	21	47	48	35	32	40	58	32
Sm	2.9	9.6	6.7	2.8	7.0	6.9	5.6	5.4	6.6	9.7	4.8
Eu	0.67	1.7	1.3	0.59	1.3	1.2	1.4	1.3	2.3	2.5	1.2
Gd	2.5	6.3	4.5	2.2	4.9	4.7	3.9	4.0	5.0	6.9	3.6
Tb	0.39	0.84	0.56	0.32	0.68	0.61	0.51	0.56	0.65	0.97	0.47
Dy	2.4	4.5	3.0	1.7	3.5	3.4	2.6	3.1	3.3	4.9	2.6
Ho	0.49	0.85	0.54	0.35	0.63	0.62	0.50	0.60	0.59	0.90	0.51
Er	1.5	2.4	1.5	1.1	1.7	1.8	1.4	1.7	1.5	2.4	1.5
Tm	0.23	0.37	0.22	0.18	0.24	0.26	0.22	0.27	0.23	0.35	0.25
Yb	1.5	2.3	1.2	1.2	1.3	1.4	1.4	1.7	1.4	2.3	1.7
Lu	0.20	0.32	0.20	0.22	0.19	0.21	0.21	0.27	0.20	0.32	0.27
Hf	3.7	7.6	6.1	3.7	5.4	4.1	4.7	4.2	4.5	6.4	5.3
Ta	0.81	2.1	1.1	1.3	1.4	1.7	0.75	0.74	0.79	1.3	0.94
Pb	28	17	23	31	25	30	21	25	17	15	20
Th	14	19	21	25	14	16	12	13	4.9	7.5	19
U	1.2	1.7	2.3	4.6	1.1	2.1	2.2	1.8	1.1	1.6	3.7
$(La/Yb)_N$	15	35	52	26	46	42	26	21	24	20	22
$(Dy/Yb)_N$	1.1	1.3	1.7	0.94	1.80	1.6	1.2	1.2	1.6	1.4	1.0
$(Gd/Yb)_N$	1.4	2.3	3.1	1.5	3.1	2.8	2.3	1.9	3.0	2.5	1.8
Sr/Y	17	21	41	15	23	25	47	32	60	34	36

SiO_2	76.60	56.14	56.06	57.27	70.44	61.44	77.49	48.81	56.49	47.90
TiO_2	0.109	0.801	0.866	0.955	0.402	0.754	0.074	1.382	1.184	2.092
Al_2O_3	12.31	15.99	14.37	15.72	14.54	15.52	12.00	16.34	18.00	17.12
Fe_2O_3t	0.78	7.93	8.28	7.65	2.69	5.81	0.71	9.40	7.52	11.59
MnO	0.023	0.131	0.135	0.123	0.052	0.097	0.027	0.136	0.143	0.125
MgO	0.04	4.55	5.70	3.80	1.07	2.81	0.04	6.42	3.07	4.06
CaO	0.58	7.25	6.80	6.00	2.32	4.78	0.18	7.59	5.26	6.61
Na_2O	3.65	3.32	3.02	3.32	3.88	3.18	4.00	4.06	5.60	4.41
K_2O	4.78	2.71	2.71	3.39	4.30	3.54	4.45	2.53	1.83	2.88
P_2O_5	0.011	0.269	0.276	0.325	0.143	0.194	0.011	0.679	0.591	0.950
LOI								1.27		
Sum	98.88	99.09	98.22	98.55	99.84	98.13	98.98	98.62	99.69	97.74
Mg#	9	53	58	50	44	49	10	58	45	41
Rb	181	92	105	117	161	103	330	89	162	109
Sr	22	793	581	697	425	611	3.30	1636	583	1214
Y	3.1	20	21	21	13	18	17	23	31	24
Zr	64	113	205	216	183	160	96.8	298	314	291
Nb	12	8.7	11	12	12	11	48	11	28	16
Cs	3.0	5.5	8.1	5.8	4.0	3.9	6.9	3.1	10	2.6
Ba	30	1518	1280	2026	944	2012	16	1646	388	1959
La	47	41	45	47	53	45	19	56	94	80
Ce	58	76	84	88	88	80	37	110	190	171
Pr	3.9	8.4	9.1	9.6	8.5	8.3	3.8	13	20	20
Nd	9.0	31	34	35	28	29	12	51	67	78
Sm	0.58	5.5	5.9	6.0	4.1	5.1	2.4	8.9	10	13
Eu	0.061	1.5	1.3	1.4	0.93	1.4	0.060	2.8	2.2	3.6
Gd	0.45	4.4	4.5	4.6	3.0	3.8	1.9	6.6	7.5	9.9
Tb	0.072	0.63	0.64	0.65	0.41	0.54	0.38	0.86	1.0	1.2
Dy	0.36	3.4	3.6	3.6	2.2	3.0	2.4	4.5	5.2	5.7
Ho	0.087	0.68	0.71	0.74	0.41	0.61	0.52	0.84	1.0	0.86
Er	0.29	1.9	2.0	2.0	1.2	1.7	1.7	2.2	2.7	2.0
Tm	0.082	0.28	0.31	0.31	0.18	0.26	0.31	0.32	0.42	0.23
Yb	0.71	1.8	1.9	1.9	1.3	1.7	2.2	1.9	2.8	1.1
Lu	0.16	0.27	0.29	0.29	0.20	0.26	0.30	0.29	0.44	0.14
Hf	3.2	3.0	5.3	5.4	4.9	4.1	4.8	6.5	7.8	6.0
Ta	0.70	0.59	0.76	0.82	1.1	0.80	3.4	0.61	2.1	0.63
Pb	33	23	24	25	23	22	28	17	18	16
Th	47	13	16	17	27	13	32	6.6	16	4.3
U	11	2.7	3.3	3.4	3.5	2.6	4.0	1.9	5.0	0.84
$(La/Yb)_N$	47	16	17	18	29	19	6.2	21	24	52
$(Dy/Yb)_N$	0.34	1.3	1.3	1.3	1.1	1.2	0.73	1.6	1.2	3.5
$(Gd/Yb)_N$	0.52	2.0	2.0	2.0	1.9	1.8	0.71	2.9	2.2	7.4
Sr/Y	7.1	40	28	33	33	34	0.19	71	19	51

$Eu^* \geqslant 1.0$ $(Eu/(Sm \cdot Gd)^{1/2}$, normalized to chondrite values), higher than normal granitoids at a given SiO_2 content (Fig. 4G). Sample 07LD-4 is relatively depleted in light REE. The Fuziling samples are characterized by their low REE contents and strong positive Eu anomalies. This indicates that the Fuziling samples and sample 07LD-4 may have a very specific petrogenesis which will be discussed separately.

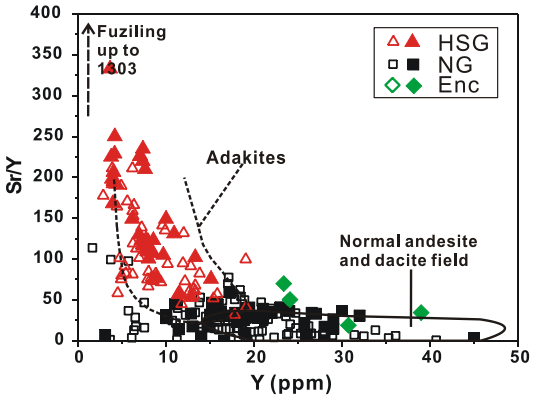

Fig. 2. Sr/Y versus Y diagram for adakites (Defant and Drummond, 1990). Closed symbols represent samples from this study; open symbols are from the literature (Chen et al., 2002; Zhang et al., 2002; Bryant et al., 2004; Qian et al., 2004; Zhao et al., 2004; Xu et al., 2005, 2007; Xie et al., 2006; Wang et al., 2007a). HSG, NG, and Enc represent high Sr/Y granitoids, normal granitoids, and dark enclaves.

In a trace element spider diagram (Fig. 4B), normal granitoids show enrichment of large ion lithophile elements (LILE, e.g., Th, U, and Pb) and depletion in high field strength elements (HFSE, e.g., Nb, Ta, and Ti). HSG also display similar enrichments of Th, U and Pb and depletions of HFSE compared to normal granitoids (Fig. 4D). However, the HSG generally have positive Sr-anomalies while normal granitoids do not. Furthermore, the HSG generally are depleted in Rb and have low Rb/Ba ratios (Fig. 4D and H), which is a typical feature of the lower continental crust (Rudnick and Gao, 2003). Although most normal granitoids with low SiO_2 have low Rb/Ba similar to the HSG, normal granitoids with high SiO_2 (e.g., >64.0%) generally have Rb/Ba ratios significantly higher than the HSG (Fig. 4B and H).

As summarized in Fig. 5, HSG and normal granitoids in the Dabie orogen can be distinguished by their distinct features in major and trace element compositions:

(1) In a Sr versus SiO_2 diagram (Fig. 5A), the HSG and normal granitoids define two separate negative correlation trends with different slopes. At a given SiO_2 content, HSG have higher Sr contents and a steeper

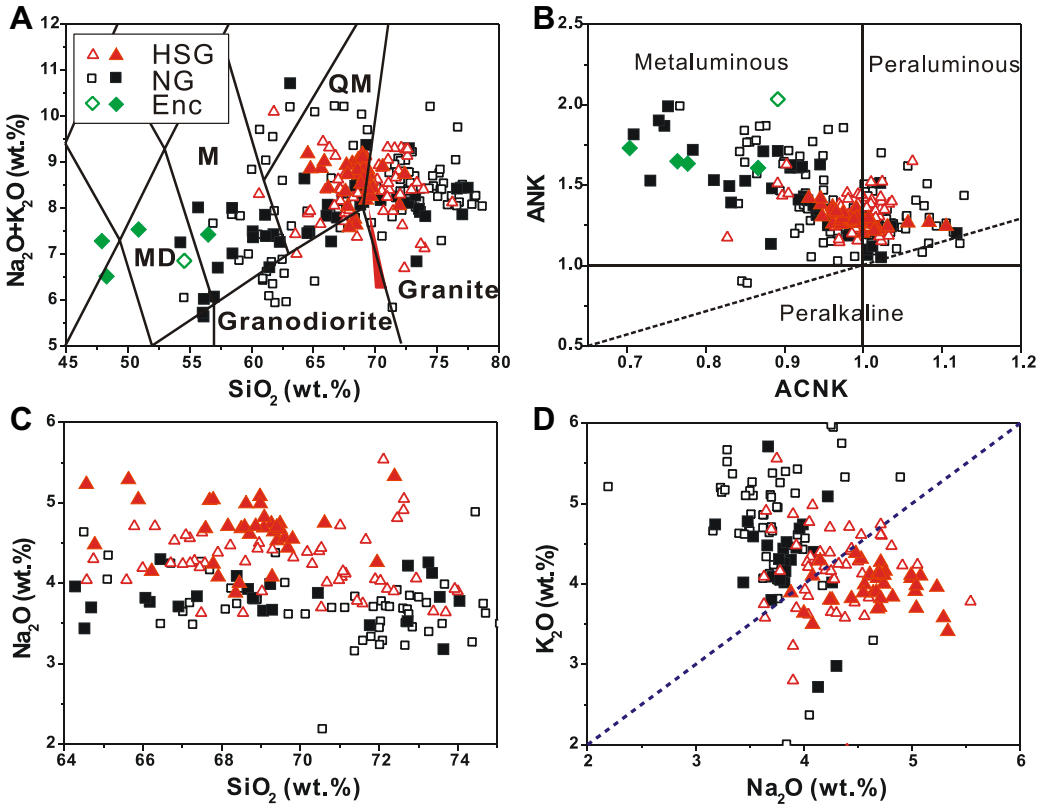

Fig. 3. Total alkali versus SiO_2 (Irvine and Baragar, 1971; Middlemost, 1985), ANK versus ACNK, and major element Harker diagrams. ANK and ACNK are molar ratios of $Al_2O_3/(Na_2O + K_2O)$ and $Al_2O_3/(CaO + Na_2O + K_2O)$, respectively. Data sources and symbols as in Fig. 2. M, MD and QM are abbreviations for monzonite, monzodiorite and quartz monzonite, respectively.

slope than normal granitoids. Similarly, the HSG and normal granitoids also define two different positive correlation trends in the Sr versus CaO diagram (Fig. 5B).

(2) Sr/Y of the HSG are correlated with $(La/Yb)_N$ (Fig. 5C, D), like adakites in modern arcs (Moyen, 2009), while normal granitoids show no clear correlation between Sr/Y and $(La/Yb)_N$ (Fig. 5D).

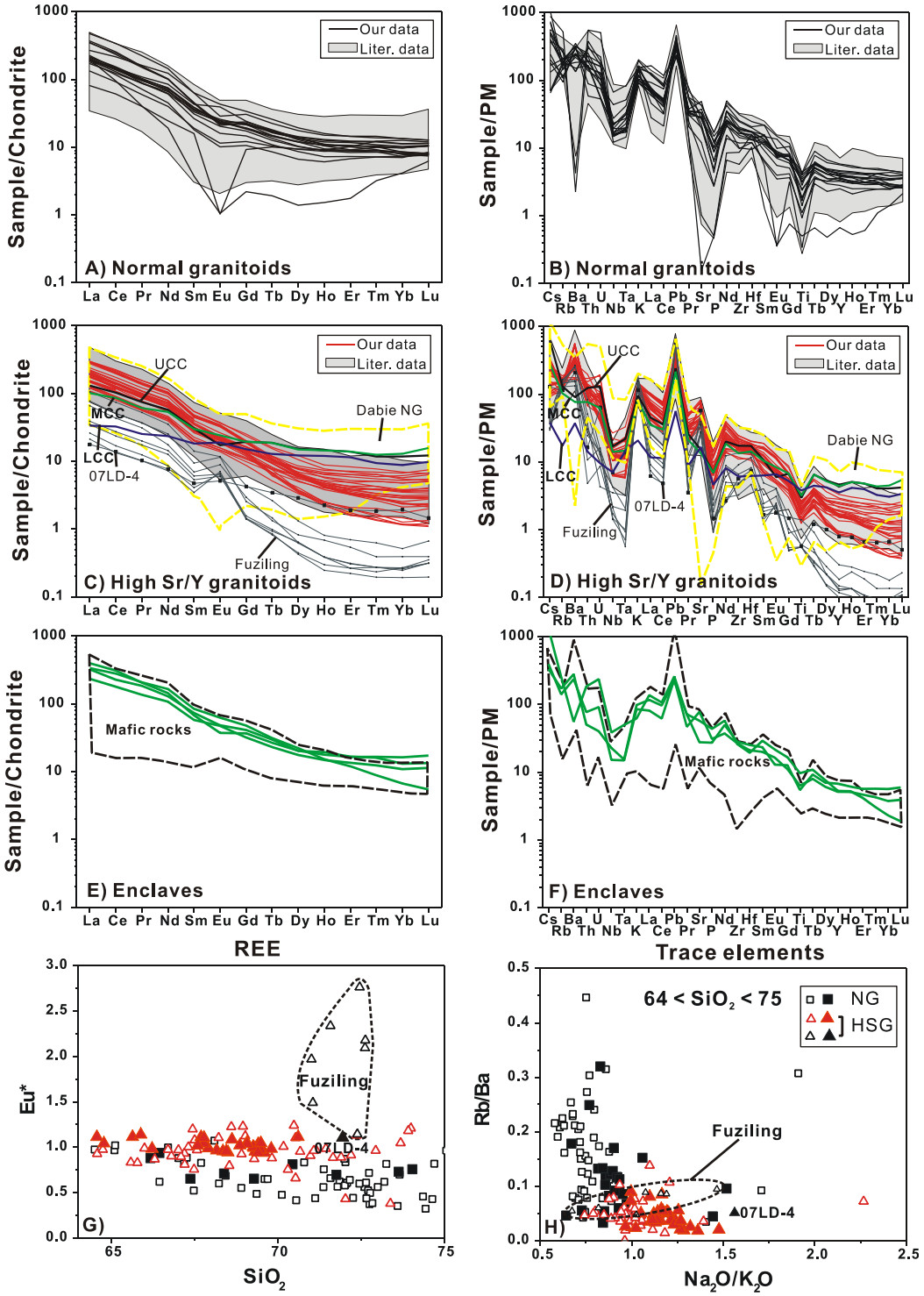

Fig. 4. Chondrite normalized REE and primitive mantle (Sun and McDonough, 1989) normalized trace element pattern for normal granitoids (NG) (A and B), 4C and 4D for high Sr/Y granitoids (HSG), and 4E and 4F for enclaves. Shown are only LA-ICPMS data. The literature data for granitoids are from sources as in Fig. 2. Contemporaneous mafic rocks are from Wang et al. (2005), Zhao et al. (2005) and Huang et al. (2007). Also shown are diagrams of Eu^* ($Eu/(Sm{\cdot}Gd)^{1/2}$, normalized to chondrite values) versus SiO_2 (G), Rb/Ba versus Na_2O/K_2O (H).

(3) HSG define a positive correlation between $(La/Yb)_N$ and $(Dy/Yb)_N$ while normal granitoids overlap in the lower part of the HSG trend (Fig. 5E). Furthermore, although both show fractionated REE patterns, the HSG have variably higher $(La/Yb)_N$ (20–151) and $(Dy/Yb)_N$ (1.0–3.2) than normal granitoids, which have $(La/Yb)_N$ from 2.5 to 52 and $(Dy/Yb)_N$ from 0.34 to 1.9 (Fig. 5E).

(4) In the Nb/Ta versus $(Dy/Yb)_N$ diagram (Fig. 5F), the HSG define a positive correlation between Nb/Ta and $(Dy/Yb)_N$ whereas normal granitoids do not. Furthermore, the HSG show variable and high Nb/Ta ratios relative to normal granitoids. Nb/Ta in HSG vary from 13 to 20 with an average of 16; normal granitoids from 11 to 17 with an average of 14.

Fuziling samples and sample 07LD-4 show different trace element correlations (Fig. 5C and E). At a given $(La/Yb)_N$, Fuziling samples and sample 07LD-4 have relatively higher Sr/Y than the HSG trend (Fig. 5C). Fuziling samples show lower $(Dy/Yb)_N$ relative to the HSG trend at a given $(La/Yb)_N$ (Fig. 5E).

Fig. 6 shows that Sr/Y, Sr/CaO, $(La/Yb)_N$, and $(Dy/Yb)_N$ ratios of the HSG are significantly higher than normal granitoids and they do not exhibit correlation with SiO_2, while the normal granitoids show slightly negative correlation trends between SiO_2 and Sr/Y, $(Dy/Yb)_N$.

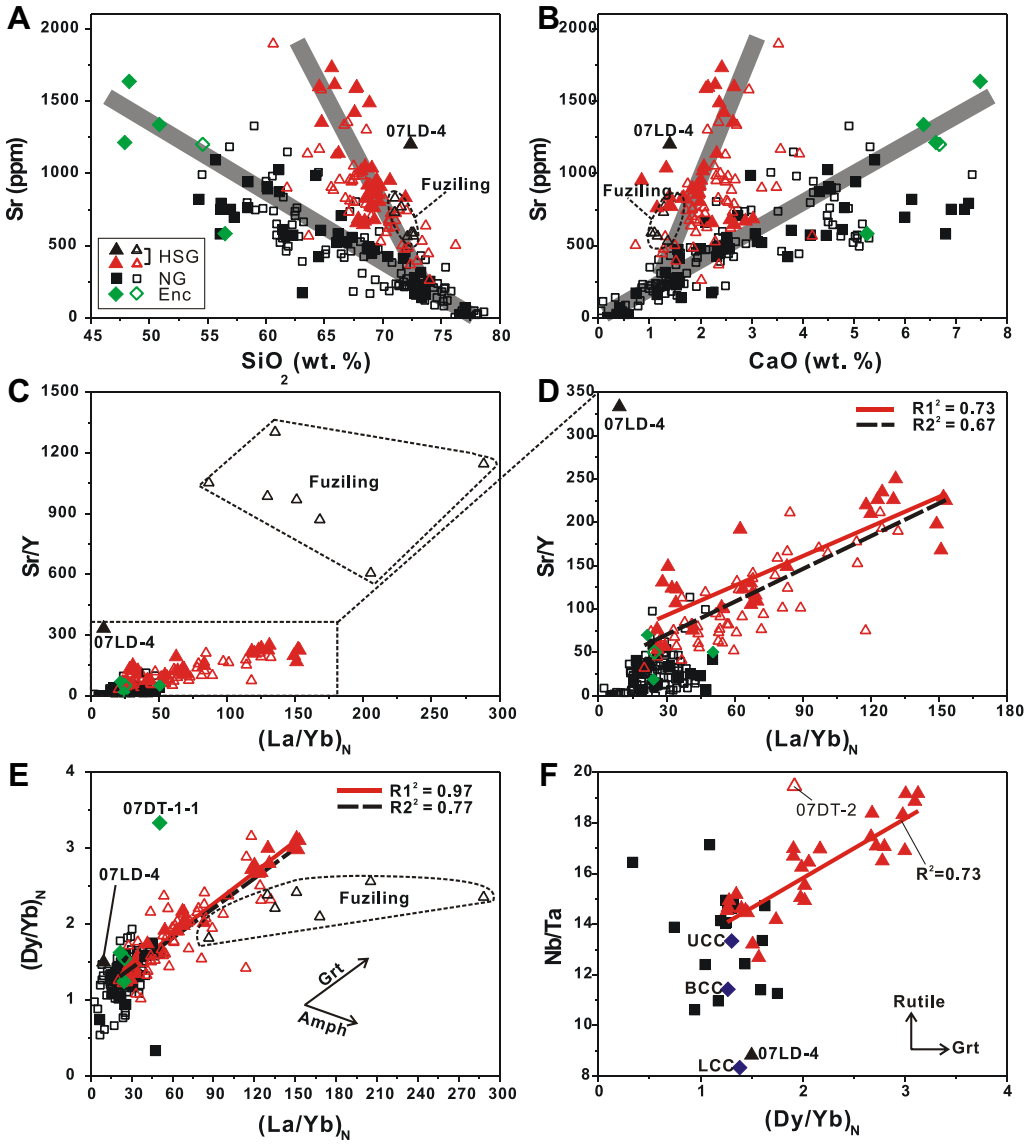

Fig. 5. Selected geochemical parameters of high Sr/Y granitoids relative to normal granitoids (subscript N means normalization to CHUR, Sun and McDonough, 1989). Data sources and symbols are similar to Fig. 2. Lines in DEF were acquired for HSG, except the Fuziling samples and sample 07LD-4, by linear fitting using OriginPro 8.0. Only our data are used for the solid lines, whereas both our and literature data are used for the dashed lines. Our data only are plotted in F, as the literature data show a much larger variation in Nb/Ta ratios (5.1–65), possibly indicating less precise measurements, compared to our data (8.8–20). For the fitting line in F, sample 07DT-2 is regarded as an outlier.

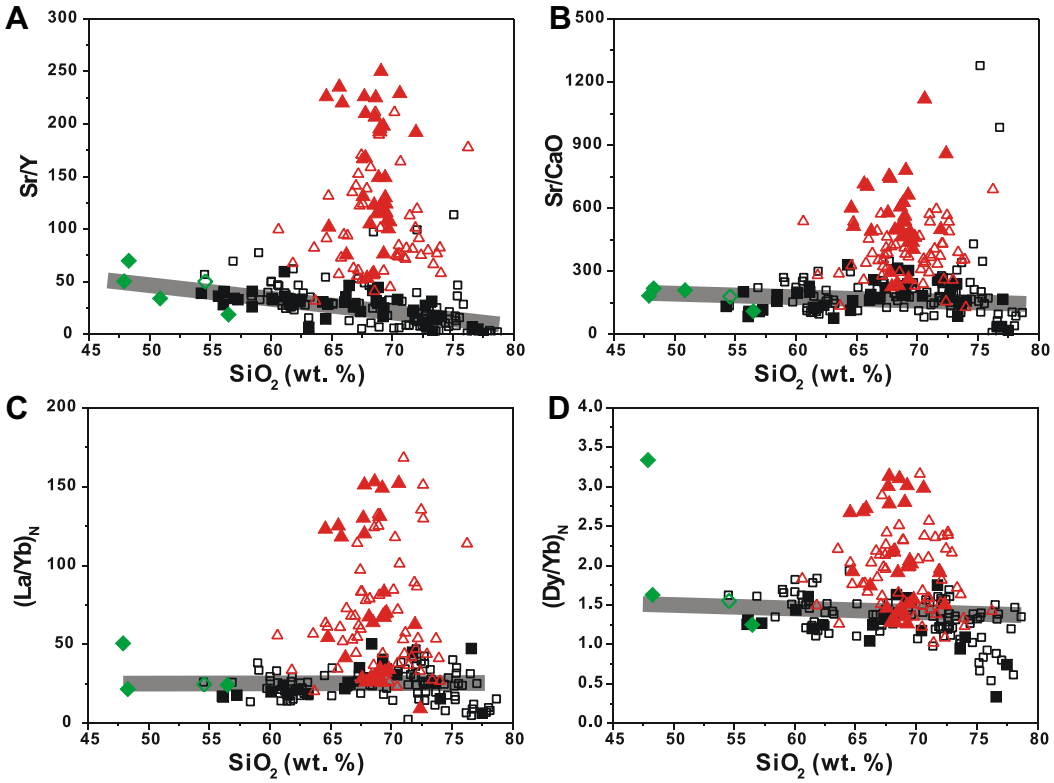

Fig. 6. Sr/Y, $(Dy/Yb)_N$, $(La/Yb)_N$, and Sr/CaO versus SiO_2. Data sources and symbols are from sources as in Fig. 2. The Fuziling samples and sample 07LD-4 are not included.

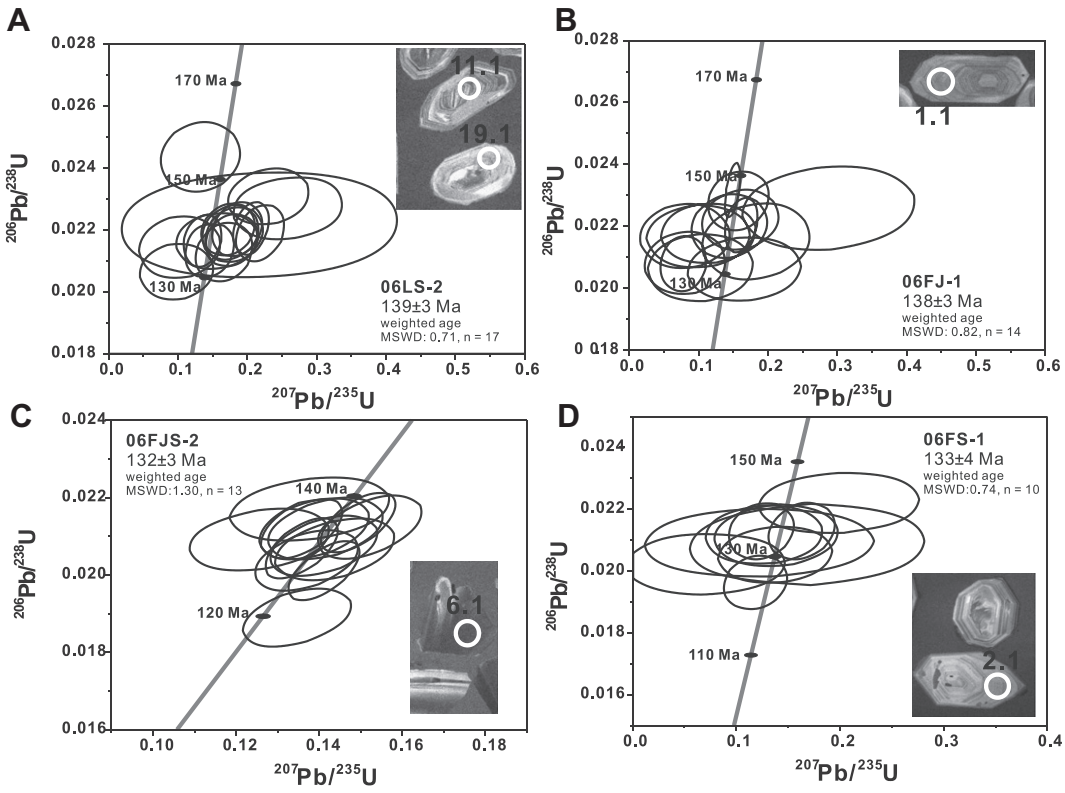

Fig. 7. SHRIMP zircon U–Pb concordia diagrams with CL images of zircons for samples 06LS-2 (Liangshan) (A), 06FJ-1 (Shangcheng) (B), 06FJS-2 (Fujinshan) (C), and 06FS-1 (Fushan) (D). Numbers on the CL images are spot numbers from Table C2.

Melanocratic enclaves, being mostly mafic (4 of 5), have compositions from foid gabbro, monzodiorite, to monzonite with SiO_2 from 47.9 to 56.5 wt% (Fig. 3A). Melanocratic enclaves have moderate to high Sr contents (583–1636 ppm) and Y contents (>23 ppm). Their REE and spider patterns are similar to those from contemporaneous mafic intrusions in the Dabie orogen, showing fractionated REE, enrichment of LILE, and depletion of HFSE (Fig. 4E and F). Melanocratic enclaves follow the trends of normal grantoids in Figs. 5 and 6, however, 07DT-1-1 has an unusually high $(Dy/Yb)_N$.

4.2. Geochronology

Zircons from two HSG (06LS-2, Liangshan; 06FJ-1, Shangcheng) and two normal granitoids (06FJS-2, Fujinshan; 06FS-1, Fushan) are generally subhedral to euhedral, prismatic, colorless, and transparent. CL images reveal core-rim structures in a quarter to a third of all grains from 06LS-2 and 06FJ-1. The rims and grains without core-rim structures display oscillatory zoning and most of them have high Th/U ratios (0.32–1.99) (Appendix C, Table C2), which is typical for magmatic zircons. 17 analyses of magmatic zircons for 06LS-2 yield $^{206}Pb/^{238}U$ ages from 132 to 155 Ma, with a weighted mean of 139 ± 3 Ma (2σ error) and 14 analyses of 06FJ-1 from 132 to 148 Ma, with a weighted mean age of 138 ± 3 Ma (2σ error) (Fig. 7A and B). In addition, four inherited zircon cores from 06LS-2 yield two concordant (201 ± 6 and 1819 ± 23 Ma) ages and two discordant (218 ± 6 and 2093 ± 37 Ma) ages (Appendix C, Table C2). Two inherited zircon cores from 06FJ-1 yield one concordant (998 ± 22 Ma) age and one discordant (2727 ± 13 Ma) age (Appendix C, Table C2). Thirteen analyses of magmatic zircons from 06FJS-2 yield a weighted mean age of 132 ± 3 Ma and 10 analyses of magmatic zircons from 06FS-1 yield a weighted mean age of 133 ± 4 Ma (2σ error) (Fig. 7C and D). No inherited zircons have been found in the two normal granitoid samples. In summary, the HSG (138–139 Ma) are slightly older than the normal granitoids (132–133 Ma), consistent with previous observations (Wang et al., 2007a; Xu et al., 2007).

5. DISCUSSION

5.1. Petrogenesis of the Dabie high Sr/Y grantoids

The high Sr/Y granitoids (HSG) in the Dabie orogen have Sr/Y and Y comparable to adakites (Defant and Drummond, 1990). An important question then is, whether they represent products of partial melting of thickened LCC with garnet dominant and plagioclase more or less absent in the residue or whether they are derived (i) from magma mixing (Chen et al., 2004; Guo et al., 2007), (ii) from fractional crystallization of Y-enriched minerals (Richards and Kerrich, 2007), or iii) from melting of high Sr/Y sources (Kamei et al., 2009; Zhang et al., 2009). As our study reveals a distinct chemistry of HSG relative to normal granitoids, it may provide new constraints on all aspects of granitoid petrogenesis.

5.1.1. Magma mixing and fractionation?

Mafic enclaves, present in some HSG and normal granitoid plutons, generally fall in the normal granitoid fields (see Figs. 5 and 6). Large variations of Sr/Y, Sr/CaO, $(Dy/Yb)_N$, $(La/Yb)_N$, and Nb/Ta (7.9, 8.7, 3.2, 7.6, and 1.5 times, respectively) are found in the HSG at similar SiO_2 contents; no strong correlation of these ratios with SiO_2 has been observed (Fig. 6). The lack of variation with SiO_2 content does not support the notion that the variations and the trends among these ratios are produced by magma mixing. It can also be precluded that compositional variations of the HSG result from fractional crystallization, because fractional crystallization would produce strong correlation trends with SiO_2 (e.g., Macpherson et al., 2006). Thus, HSG represent initial magmas with variably higher Sr, Sr/CaO, Sr/Y, $(Dy/Yb)_N$, $(La/Yb)_N$, and Nb/Ta than normal granitoids.

Indicated by the preservation of a high positive correlation between $(Dy/Yb)_N$ and $(La/Yb)_N$, fractional crystallization of amphibole is not a significant process for most HSG. Generally, amphibole favors middle and to a lesser extent heavy REE relative to light REE (e.g., Nash and Crecraft, 1985; Green, 1994; Brenan et al., 1995). Thus a negative correlation between $(Dy/Yb)_N$ and $(La/Yb)_N$ is expected for fractional crystallization. Also, fractional crystallization of a substantial amount of plagioclase would produce negative Eu anomalies (e.g., Drake, 1976; Bindeman and Davis, 2000; Bedard, 2006), which are not observed in most HSG. In summary, we conclude that fractional crystallization is not significant for most HSG.

The Fuziling samples are characterized by depleted REE and Y and generally high Sr/Y ratios (up to 1303) relative to the other HSG (Wang et al., 2007a). Due to decreasing La contents as P_2O_5 decreases and increasing Sr/Y as La contents decrease (Table 2 in Wang et al., 2007a), this feature can be explained by apatite and/or monazite fractionation in the Fuziling samples. Using partition coefficients for granites from Bea et al. (1994), fractionation of ca. 0.7% apatite or ca. 0.025% monazite only can account for the range of Y (from 1.4 to 0.45 ppm). A similar effect is observed for 07LD-4 with its depleted LREE (Fig. 4C). A depletion of LREE in the other HSG has not been observed, suggesting fractional crystallization of apatite and/or monazite is not important for most HSG.

Finally, fractional crystallization of zircon can elevate both $(La/Yb)_N$ and $(Dy/Yb)_N$ (e.g., Bea et al., 1994), and titanite, favoring Ta (Prowatke and Klemme, 2005), can fractionate Nb and Ta. However, these two minerals are commonly present both in HSG and normal granitoids (Table A1). Furthermore, no correlations between $(Dy/Yb)_N$ and Zr contents, Nb/Ta and TiO_2 are observed. Therefore, zircon and titanite may not account for the distinct high $(Dy/Yb)_N$ and Nb/Ta of HSG in contrast to normal granitoids.

5.1.2. A high Sr/Y source for HSG at low pressure?

Moyen (2009) proposed that the lower continental crust (LCC) may have high Sr/Y up to 80 (Weaver and Tarney, 1984), and thus any melt from the LCC might have Sr/Y > 40. However, most LCC estimates indicate an average

Table 2
Partition coefficients and presumed source for trace element modeling. The LCC estimate of Rudnick and Gao (2003) has been taken as presumed source (PS). Selected partition coefficients are from felsic magmas; and from experimental runs under equilibrium conditions similar to HSG if possible. For example, D_{REE} for garnet and clinopyroxene are from an experimental run at 1050 °C, 1.5 GPa (Klein et al., 2000). Data sources for partition coefficients are: REE, Nb, and Ta for garnet and clinopyroxene, from Klein et al. (2000); for Y estimates of the average of Dy and Er; Sr for garnet from Pertermann et al. (2004); Sr for clinopyroxene from Huang et al. (2006); Nb and Ta for rutile from Klemme et al. (2005). Representative calculations are listed for batch melting and fractional melting with residue as 30% garnet + 69% clinopyroxene + 1% rutile (*). One of most distinct HSG (07LS-2) is also shown for comparison.

Element	PS	Partition coefficients					
	LCC	Grt	Cpx	Rutile	Bulk D (30:69:1)*		
Sr	348	0.013	0.39		0.273		
Y	16	7.7	1.55		3.38		
La	8	0.025	0.099		0.076		
Dy	3.1	4.4	1.2		2.15		
Yb	1.5	14	0.9		4.82		
Nb	5	0.04	0.005	96	0.975		
Ta	0.6	0.08	0.014	210	2.13		
Batch melting							
Melt fraction	5	10	15	20	25	30	07LS-2
Sr	1125	1007	911	832	765	709	841
Y	4.91	5.09	5.29	5.51	5.75	6.00	3.7
La	65.6	47.6	37.3	30.7	26.1	22.7	42
Dy	1.48	1.52	1.57	1.62	1.67	1.72	0.91
Yb	0.32	0.34	0.35	0.37	0.39	0.41	0.20
Nb	5.12	5.11	5.11	5.10	5.09	5.09	4.5
Ta	0.29	0.30	0.31	0.31	0.32	0.33	0.24
Sr/Y	229	198	172	151	133	118	227
$(La/Yb)_N$	145.2	100.9	75.8	59.5	48.2	39.8	151
$(Dy/Yb)_N$	3.06	3.02	2.97	2.93	2.87	2.82	3.0
Nb/Ta	17.7	17.2	16.7	16.2	15.7	15.2	19
Nb/La	0.078	0.108	0.137	0.166	0.195	0.225	0.11
Fractional melting							
Melt Fraction	1	6	11	16	21	26	31
Sr	1241	1081	935	801	680	572	475
Y	4.77	4.95	5.14	5.35	5.59	5.85	6.15
La	93.36	49.63	25.49	12.60	5.96	2.69	1.14
Dy	1.45	1.49	1.54	1.58	1.64	1.70	1.76
Yb	0.314	0.327	0.341	0.357	0.375	0.395	0.418
Nb	5.12	5.12	5.11	5.10	5.10	5.09	5.08
Ta	0.283	0.291	0.299	0.309	0.319	0.330	0.342
Sr/Y	260	219	182	150	122	97.7	77.2
$(La/Yb)_N$	214	109	53.6	25.3	11.4	4.88	1.97
$(Dy/Yb)_N$	3.10	3.06	3.01	2.97	2.92	2.87	2.82
Nb/Ta	18.1	17.6	17.1	16.5	16.0	15.4	14.8
Nb/La	0.055	0.103	0.200	0.405	0.855	1.89	4.44

LCC with Sr/Y $\leqslant$ 28 (7–28, $n = 11$, Table 7 in Rudnick and Gao (2003) and references therein). Furthermore, the LCC has an average $(Dy/Yb)_N$ composition of $\leqslant$1.6 (Rudnick and Gao, 2003). Local basement rocks, which mainly consist of high to ultrahigh pressure metamorphic rocks with Neoproterozoic protolith ages (Zheng et al., 2003), also have relatively low $(Dy/Yb)_N$ (Fig. 8A). At low pressures, melting of LCC with clinopyroxene (or amphibole) as dominant residual phases may produce granitoids with high Sr/Y but low $(Dy/Yb)_N$. This disagrees with high Sr/Y up to 282 together with high $(Dy/Yb)_N$ of the HSG.

It is also important to examine whether the chemical features of the HSG are inherited from their source rocks, such as old adakites or TTG suites (Kamei et al., 2009; Zhang et al., 2009). As shown in Fig. 8B, at a given CaO content, the Dabie HSG have higher Sr concentrations than most adakites in modern arcs (GeoRoc; http://georoc.mpch-mainz.gwdg.de/) and high Sr/Y TTG, including a global compilation from Condie (2005) and Kongling TTG gneisses from South China Block (Gao et al., 1999; Ma et al., 2000; Zhang et al., 2006). Given intermediate to felsic compositions, melting of TTG or adakite sources fails to produce as high Sr concentrations as the Dabie HSG at a given CaO content, because feldspar is an important residual phase at pressures up to 3.0 GPa (e.g., Patino Douce, 2005; Watkins et al., 2007). Furthermore, most global high Sr/Y TTG suites, including the Kongling TTG, and adakites in modern arcs display smaller variations in

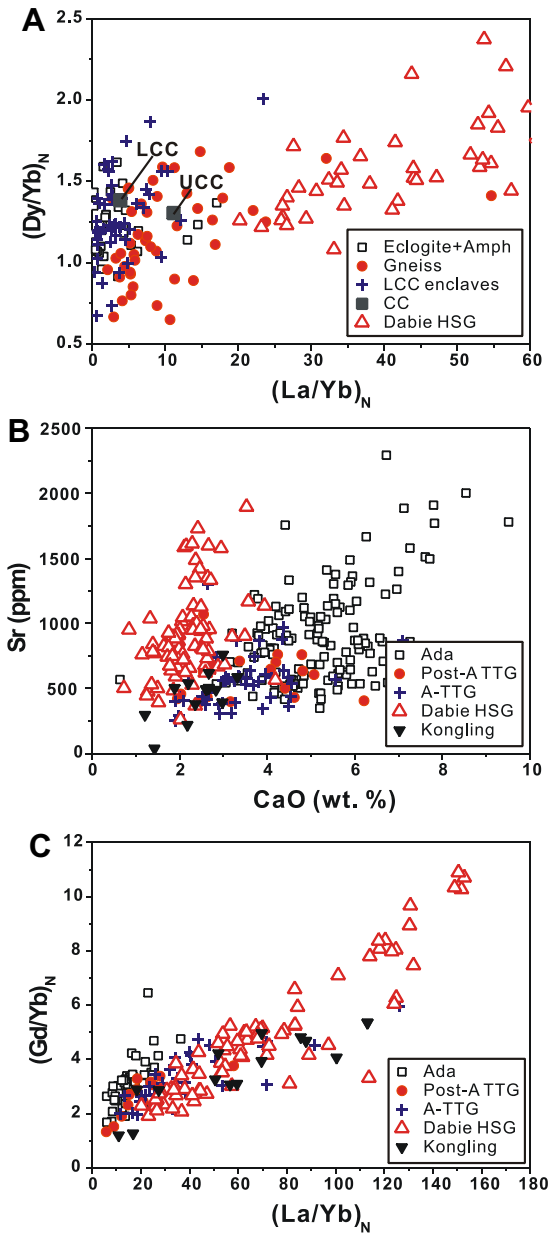

Fig. 8. $(Dy/Yb)_N$ versus $(La/Yb)_N$ (A), Sr versus CaO (B), and $(Gd/Yb)_N$ versus $(La/Yb)_N$ (C) of Dabie HSG, local basement, global mafic lower continental crustal xenoliths, high Sr/Y TTG suites, and adakites in modern arcs. (A) Eclogite + Amph, Gneiss: eclogites + amphibolites and gneisses in local basement, LCC enclaves: global mafic lower continental crustal xenoliths, and CC: average composition of continental crust (Rudnick and Gao, 2003). (B and C) Ada, adakites in modern arcs; Post-A TTG, post-Archean high Sr/Y TTG suites; A-TTG, Archean high Sr/Y TTG suites; and Kongling, Kongling TTG. Local exposed basement represent amphibolites, eclogites, and gneisses with Neoproterozoic protolith ages (Li et al., 2000; Bryant et al., 2004; Zhao et al., 2007b; Tang et al., 2008; Xia et al., 2008). Amphibolites and TTG gneisses of the Kongling complex are from Gao et al. (1999), Ma et al. (2000); and Zhang et al. (2006). Mafic xenoliths of lower continental crust and global high TTG suites are from the compilation of Condie (2005) and Rudnick and Gao (2003). Mafic xenoliths from kimberlites and minettes are excluded. Adakites in modern arcs are from the GeoRoc database (http://georoc.mpch-mainz.gwdg.de/) without continental settings.

$(Dy/Yb)_N$ (or $(Gd/Yb)_N$) than the HSG (Fig. 8C). Melting of such TTG or adakite sources at low pressures with clinopyroxene and amphibole as the dominant mafic residual phases will not produce magmas with substantially higher $(Dy/Yb)_N$ or $(Gd/Yb)_N$. For example, although high Sr/Y granitoids reported by Zhang et al. (2009) have high Sr/Y and La/Yb ratios, their $(Dy/Yb)_N$ values are generally lower than 1.4, which is much lower than the supposed TTG protolith with $(Dy/Yb)_N$ up to 2.9 (Figs. 8C and 11E). Therefore, high $(Dy/Yb)_N$ up to 3.2, and the high Sr concentrations in the Dabie HSG argue against the inheritance of their source compositions at low pressure.

5.1.3. Intermediate-felsic or mafic source for the Dabie HSG?

Felsic HSG in the Dabie orogen have been interpreted as partial melts from thickened intermediate to felsic crust (Xu et al., 2008). However, Wang et al. (2007a) suggested that the Dabie HSG are most likely derived from partial melting of metabasalts. Vapor-absent partial melting experiments of intermediate to felsic rocks (SiO_2 = 59–70%, A/CNK = 0.90–1.04) show that low to high degrees (7–60%) of partial melts at pressures from 1.0 to 3.0 GPa have highly variable A/CNK from 1.03 to 2.07 and SiO_2 >70% (Skjerlie and Johnston, 1996; Patino Douce, 2005; Watkins et al., 2007). These experiments also show that feldspar is a dominant residual phase at pressures up to 3.0 GPa and melt fractions up to 60% (Skjerlie and Johnston, 1996; Patino Douce, 2005; Watkins et al., 2007). By contrast, the HSG generally have A/CNK from 0.90 to 1.10 and SiO_2 <71% (n = 70/85), which both are slightly lower than those of the partial melts from intermediate to felsic sources. Furthermore, most HSG have high Sr and Ba contents relative to normal granitoids at a given CaO content, which suggests that feldspar is not an important phase in the HSG sources. Therefore, the HSG unlikely are to be derived from intermediate to felsic sources. A/CNK ratios of ~1.0 in the HSG may be produced by partial melting of a garnet-bearing basaltic protolith at pressure–temperature conditions close to or beyond the 'amphibole-out' phase boundary, as feldspar is absent in residual phases (Rapp, 1995).

5.1.4. Partial melting of thickened continental crust

In contrast to magma mixing, fractional crystallization and source inheritance, the distinct, coupled geochemical features suggest that the Dabie HSG are derived from partial melting of a thickened mafic continental crust.

The Dabie HSG define a high Sr correlation with SiO_2 or CaO compared to normal granitoids, and have Sr concentrations even higher than adakites and Archean TTG suites at a given CaO content. Furthermore, the positive correlation between Sr/Y and $(La/Yb)_N$ indicates that Sr most likely behaves like La as an incompatible element during melting. Plagioclase, thus, was mostly absent in the residue for the HSG.

Given that garnet is the only rock-forming mineral that can substantially fractionate middle REE from heavy REE, high $(Dy/Yb)_N$ ratios may better reveal the involvement of garnet than high Sr/Y and $(La/Yb)_N$ (Huang and He, 2010). Furthermore, as D_{REE} values increase with atomic numbers, garnet is the only rock-forming mineral that can

substantially enhance both $(La/Yb)_N$ and $(Dy/Yb)_N$ (or $(Gd/Yb)_N$) of magmas (e.g., Blundy and Wood, 1994; Klein et al., 2000; Pertermann et al., 2004). Positively correlated high $(Dy/Yb)_N$ and $(La/Yb)_N$ ratios thus suggest the dominant role of garnet in fractionating REE of the HSG during partial melting.

Nb and Ta fractionation is governed by Ti-enriched minerals (Foley et al., 2000; Klemme et al. (2005), Prowatke and Klemme, 2005). The presence of rutile and titanite in the residue both can lead to high Nb/Ta and low Nb/La of melts (Klemme et al. (2005), Prowatke and Klemme, 2005), consistent with the negative correlation of HSG in Fig. 9. Except sample 07DT-2, for the major HSG trend, however, the variation in Nb/La (0.092–0.39) is much higher than that of Nb/Ta (13–19) (Fig. 9), inconsistent with the effect of titanite. For dacitic to rhyolitic melts, D_{Nb}/D_{La} of titanite ranges from 2.9 to 3.3, while D_{Nb}/D_{Ta} ranges from 0.09 to 0.10, respectively (Prowatke and Klemme, 2005). Accordingly, the fractionation of Nb/Ta is much larger than that of Nb/La when titanite is present. By contrast, La is highly incompatible, whereas Nb is compatible in rutile with D_{Nb} up to 96, resulting in $D_{Nb}/D_{La} >> 96$. D_{Nb}/D_{Ta} of rutile ranges from 0.21 to 0.46 (Klemme et al., 2005). Rutile, thus, can both explain the larger variation in Nb/La than Nb/Ta and the slightly elevated Nb/Ta ratios of the HSG relative to normal granitoids.

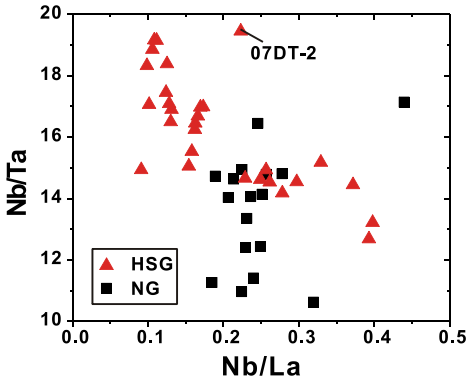

Fig. 9. Nb/Ta versus Nb/La for Dabie HSG and normal granitoids. Our data are plotted only.

Co-variations in Sr/Y, $(La/Yb)_N$, $(Dy/Yb)_N$, and Nb/Ta have been modeled on the basis of batch partial melting and fractional partial melting (Shaw, 1970). As demonstrated (e.g., Rapp et al., 1991; Sen and Dunn, 1994; Rapp, 1995; Rapp and Watson, 1995), garnet and clinopyroxene are considered to be major residual minerals with traces of co-existing rutile. The average composition of LCC (Rudnick and Gao, 2003) is taken to approximate the source composition. It should be noted that 7% tonalite gneisses and 97% mafic lithologies contribute to the estimate of LCC in Rudnick and Gao (2003). Partition

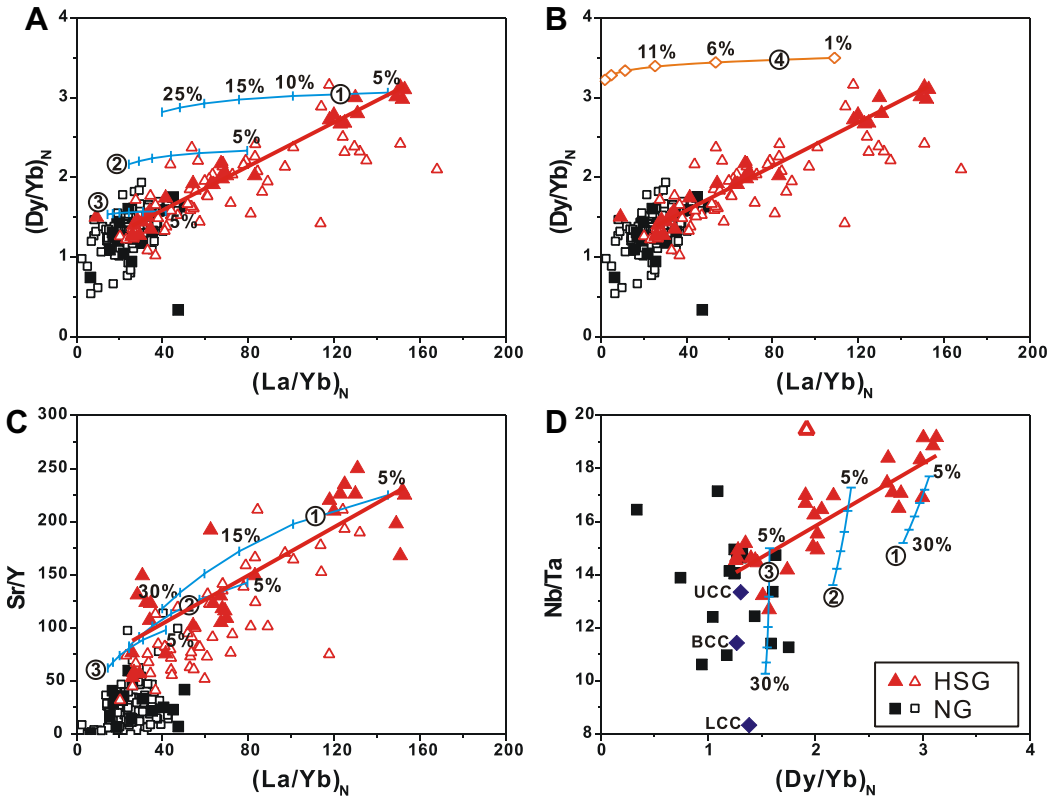

Fig. 10. Trace element modeling of partial melting of thickened LCC. Parameters are from Table 2. Curves 1, 2, and 3 are for batch partial melting with residual phases as 30% garnet + 69% clinopyroxene + 1% rutile (curve 1), 15% garnet + 84.5% clinopyroxene + 0.5% rutile (curve 2), and 5% garnet + 94.9% clinopyroxene + 0.1% rutile (curve 3), respectively. Segments on curves remark 5% increments in melt fraction. Curve 4 in B is for fractional partial melting with residual phases as 30% garnet + 69% cpx + 1% rutile. Thick red lines are from Fig. 5. (For interpretation of the references to color in this figure legend, the reader is referred to the web version of this paper.)

coefficients used in the modeling are carefully selected and listed in Table 2. Representative results, listed in Table 2 and shown in Fig. 10, indicate that $(Dy/Yb)_N$ in melt is sensitive to residual garnet/clinopyroxene ratios, but insensitive to low and intermediate degrees (1–30%) of melt fraction. Fig. 10 also shows that $(La/Yb)_N$ and Nb/Ta are sensitive to melt fractions. The high $(La/Yb)_N$ and Nb/Ta ratios of HSG suggest low degree partial melting (ca. 5%) (Fig. 10). The calculated low degrees of batch partial melting (ca. 5%) approximate the HSG trends; gradually elevated $(La/Yb)_N$, $(Dy/Yb)_N$, and Sr/Y correspond to increasing proportions of residual garnet. On the other hand, the positive correlation between Nb/Ta and $(Dy/Yb)_N$ (Fig. 10) is modeled by varying the abundances of rutile and garnet in the residue of HSG. Additional modeling using the average composition of global mafic LCC xenoliths shows that variations of presumed source composition are not sensitive for the correlations among Sr/Y, $(Dy/Yb)_N$, $(La/Yb)_N$, and Nb/Ta. Thus co-variations of Sr/Y, $(La/Yb)_N$, $(Dy/Yb)_N$, and Nb/Ta in the HSG can be explained by a change of modal proportions of residual minerals.

In summary, the HSG are most likely derived from partial melting of thickened mafic LCC leaving garnet–clinopyroxenite residuum, in which the garnet/clinopyroxene ratio varies; plagioclase is more or less absent; and rutile is present. This mineralogy indicates that during the HSG emplacement the depth of crust was >50 km (ca. 1.5 GPa) (Rapp, 1995; Rapp and Watson, 1995; Xiong et al., 2005; Wang et al., 2007a; Xu et al., 2007). This model does not explain normal granitoids which have larger variations in major elements than the HSG and very complex petrogenesis, such as partial melting of ultramafic to intermediate rocks, magma fractional crystallization, and mixing between felsic and mafic magmas (e.g., Chen et al., 2002; Wang et al., 2007a; Xu et al., 2007; Zhao et al., 2007a,c). Furthermore, garnet cannot be dominant in the formation of normal granitoids because they generally have flat middle to heavy REE patterns except a few high-silica samples having down-concave REE patterns. Garnet becomes stable at pressures >ca. 1.0–1.2 GPa for basalitic sources and at lower pressures for intermediate to felsic sources (e.g., Rapp, 1995; Rapp and Watson, 1995; Moyen and Stevens, 2006). Crustal components in normal granitoids were most likely derived from shallower depths (<ca. 40 km) of the once thickened crust (Wang et al., 2007a; Xu et al., 2007).

5.1.5. Implications of high Na_2O and Na_2O/K_2O of the HSG

Besides high Na_2O contents and Na_2O/K_2O, the HSG generally have low Rb/Ba ratios (Fig. 4H). The Rb depletion shown in Fig. 4D is a typical feature of LCC (Rudnick and Gao, 2003). By contrast, normal granitoids with SiO_2 similar to the HSG generally have high Rb/Ba ratios (Fig. 4H), typical for middle to upper continental crust (Rudnick and Gao, 2003). Given the change in source depths, different sources (low to middle continental crust) most likely contribute to the difference in Na_2O contents and Na_2O/K_2O between HSG and normal grantioids. A change of residual phases with pressure could also play an important role. As shown above, garnet and clinopyroxene

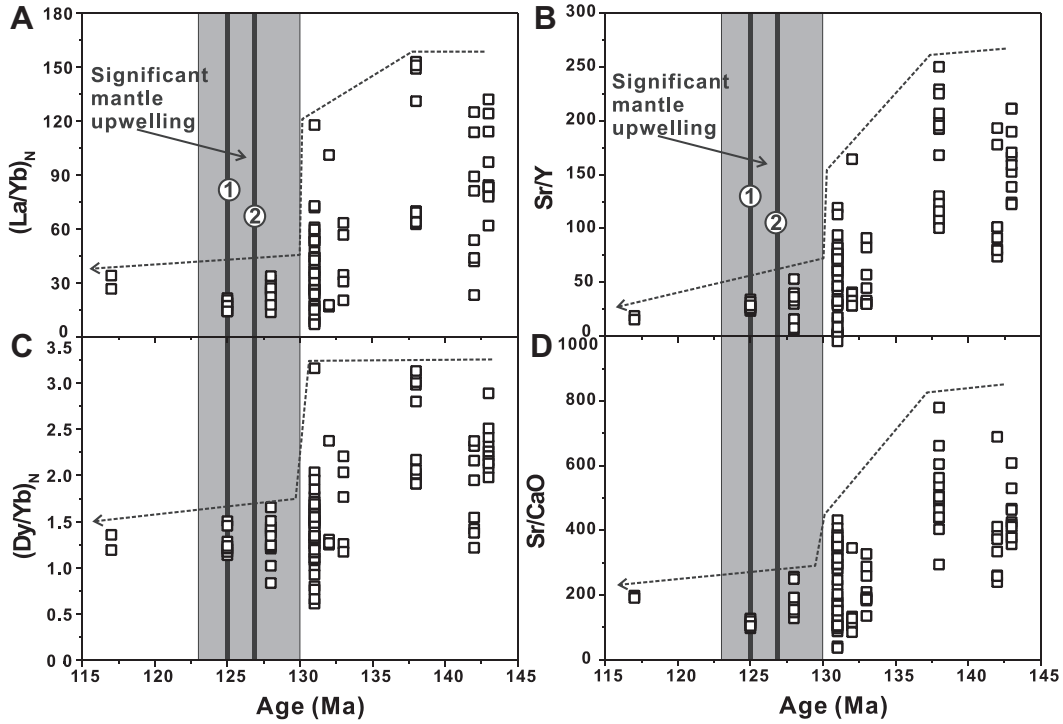

Fig. 11. Variations of $(La/Yb)_N$, $(Dy/Yb)_N$, Sr/Y, and Sr/CaO of Dabie post-collisional granitoids with age. Significant mantle upwelling is indicated by mafic–ultramafic plutons (the vertical lines 1, 2 and grey fields represent the ages and 2σ range of Shacun (125 ± 2 Ma) and Jiaoziyan (127 ± 3 Ma) plutons; Zhao et al., 2005). Data sources are the same as in Fig. 2, the age of the Fenliupu pluton is from Ma et al. (2003).

are dominant but plagioclase is more or less absent in the HSG residue, while plagioclase is a major residual phase for normal granitoids. Garnet and clinopyroxene are Na-depleted relative to plagioclase (e.g., Run B4, B5, and M2; Sen and Dunn, 1994), which results in higher Na_2O of the HSG compared to normal granitoids.

5.2. Geological implications

Interpreting most HSG as partial melts of thickened LCC in the Dabie orogen has important implications for the post-collisional tectonic evolution of the orogen. Sr/CaO, $(Dy/Yb)_N$, $(La/Yb)_N$, and Sr/Y of post-collisional granitoids in the Dabie orogen are plotted versus age (Fig. 11), showing that the distinct chemical features of partial melts of thickened LCC disappeared at ca. 130 Ma. This suggests a significant change in the crustal melting system: lacking of crustal melts from depths >ca. 50 km (plagioclase poor) since ca. 130 Ma. Seismologic investigations show that lowermost eclogitic or garnet–clinopyroxenitic LCC is lacking in the current Dabie orogen (Gao et al., 1998). Intensive magmatism in the orogen ceased at ca. 120 Ma (Wang et al., 2007a and references therein). Therefore, the eclogitic source and/or residuum of HSG were most likely removed at ca. 130 Ma. This is supported by the emplacement of the Chituling high-Mg adakitic pluton,

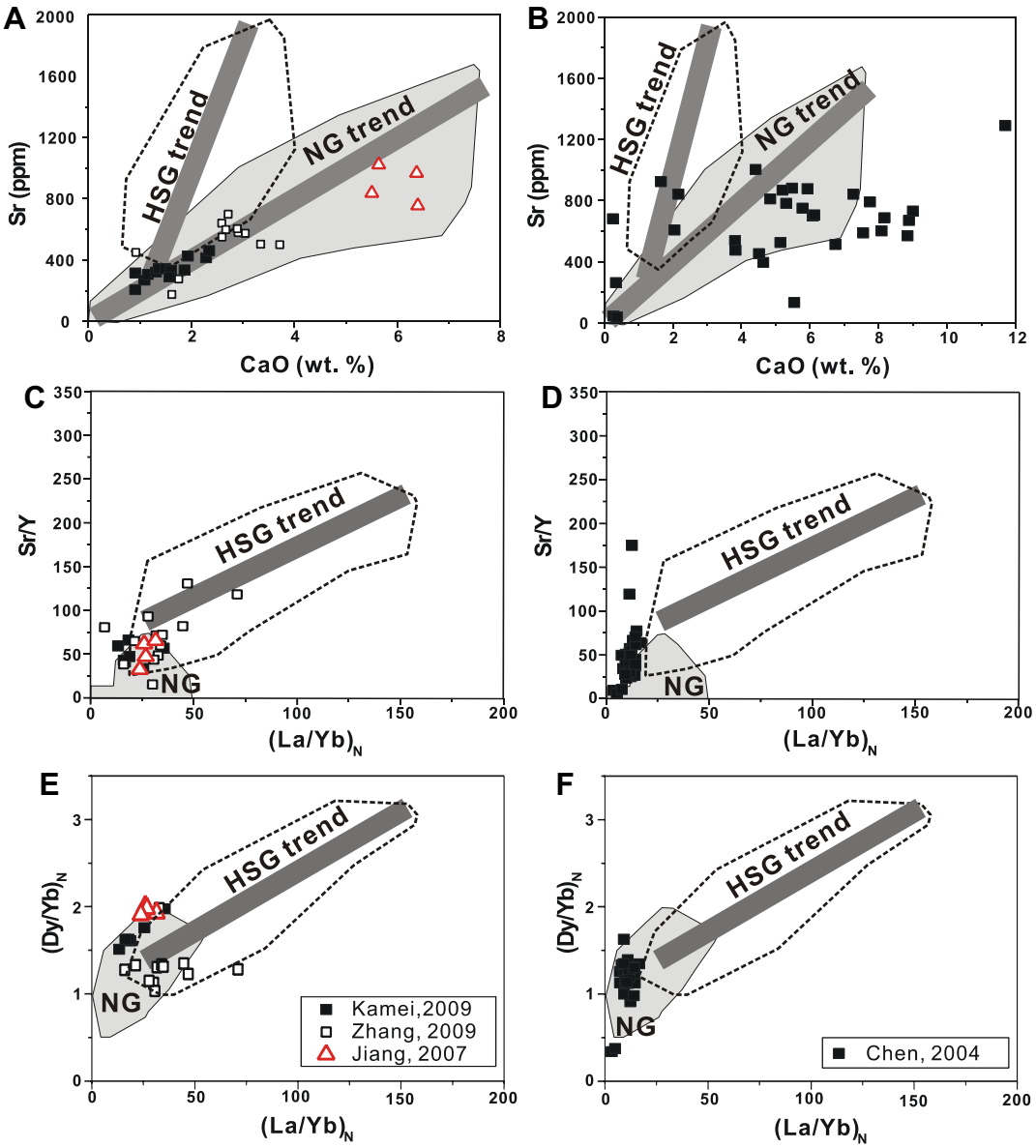

Fig. 12. Sr versus CaO (A and B), Sr/Y versus $(La/Yb)_N$ (C and D), and $(Dy/Yb)_N$ versus $(La/Yb)_N$ (E and F) for continental pseudo adakites. Supposed melts from old high Sr/Y sources without partial melting of thickened LCC are from Kamei et al. (2009) and Zhang et al. (2009) and those from partial melting of granulites are from Jiang et al. (2007) (ACE); those supposed to result from magma mixing are from Chen et al. (2004) (BDF).

regarded as partial melt of delaminated LCC (Huang et al., 2008), the emplacement of mafic and ultramafic intrusions (ca. 131–125 Ma, Li et al., 1999; Zhao et al., 2005) and a rapid crustal uplift (the Luotian dome, ca. 136–127 Ma, Hou et al., 2005) in the Dabie orogen (Kay and Kay, 1993). Initial partial melting lasts more than 10 Ma (ca. 143–130 Ma) before the thickened LCC was removed at ca. 130 Ma (Fig. 11) (Wang et al., 2007a). Partial melting of the LCC thus might support the foundering of the thickened mafic LCC because it rheologically weakened the LCC of the orogen and left a denser eclogite in the residue, triggering the mountain root removal (Wang et al., 2007a; Xu et al., 2007; Huang et al., 2008).

5.3. How to distinguish partial melts of thickened crust from pseudo-adakites?

The coupled geochemical features may have general implications to distinguish partial melts of thickened crust from high Sr/Y granitoid magmas showing no geochemical indicator of melting depths. The latter type of rocks has been termed "pseudo-adakite" by Kamei et al. (2009). Pseudo-adakites reported in the literature can be products of magma mixing, of crystal fractionation, or of partial melting of granulites, TTG suites, and adakites in normal continental crust (Chen et al., 2004; Macpherson et al., 2006; Jiang et al., 2007; Kamei et al., 2009; Zhang et al., 2009). In a Sr versus CaO diagram (Fig. 12A), those pseudo-adakites scatter along the trend defined by normal granitoids in the Dabie orogen, but do not reflect the high Sr trends of the Dabie HSG. In Sr/Y, $(Dy/Yb)_N$ versus $(La/Yb)_N$ diagrams (Fig. 12C and E), the pseudo-adakites have a much smaller range compared to Dabie HSG. Furthermore, steep positive correlations are not observed for pseudo-adakites in a $(Dy/Yb)_N$ versus $(La/Yb)_N$ diagram (Fig. 12E), except for samples reported by Kamei et al. (2009). Higher $(Dy/Yb)_N$ (1.5–2.0) of samples from Kamei et al. (2009) (Fig. 12E) cannot be explained by amphibole-dominant melting of old arc tonalites or adakites with $(Dy/Yb)_N$ between 1.2 and 1.5 as proposed by Kamei et al. (2009), because amphibole favors Dy over Yb (e.g., Green, 1994). Accordingly, it is more likely that either more garnet is present during partial melting, or the source materials have higher Dy/Yb than proposed by Kamei et al. (2009). Chen et al. (2004, 2008) suggested that some high Sr/Y igneous rocks in the Taihang orogen result from mixing of mantle and crustally derived magmas followed by fractional crystallization of clinopyroxene and amphibole. The Taihang samples form a nearly horizontal trend with the majority having low Sr at similar CaO (Fig. 12B). Furthermore, no correlations among Sr/Y, $(Dy/Yb)_N$ and $(La/Yb)_N$ have been found (Fig. 12D and F), showing a large range of Sr/Y with very limited variations in $(Dy/Yb)_N$ and $(La/Yb)_N$ which is clearly different from the case of the Dabie HSG. These features do not imply the involvement of garnet and ±absence of plagioclase, which is clearly different from the case of the Dabie HSG. Consequently, the diagrams of Sr versus CaO, and Sr/Y, $(Dy/Yb)_N$ versus $(La/Yb)_N$ can be successfully applied for the identification of partial melts of thickened crust distinguishing them from pseudo-adakites.

6. CONCLUSION

High Sr/Y granitoids (HSG) have distinct geochemical features relative to normal granitoids in the Dabie orogen. Besides high Sr/Y and low Y, the Dabie HSG have high Sr and Sr/Ca ratios, high $(Dy/Yb)_N$, $(La/Yb)_N$ and Nb/Ta ratios and define high positive correlations among Sr/Y, $(La/Yb)_N$, $(Dy/Yb)_N$, and Nb/Ta in contrast to normal granitoids. These distinct geochemical features of the HSG are best explained by partial melting of a thickened lower continental crust. Comparison of the Dabie HSG with pseudo-adakites suggests that the distinct chemical features found here can be used as additional criteria to distinguish partial melts of thickened LCC from pseudo-adakites.

Temporal variations of Sr/CaO, $(Dy/Yb)_N$, $(La/Yb)_N$ and Sr/Y for post-collisional granitoids reveal a lack of HSG since ca.130 Ma in the Dabie orogen. Combined with previous geophysical and geological studies, this suggests that the eclogitic source and/or residuum of HSG were most likely removed at that time.

ACKNOWLEDGMENTS

We thank Klaus Simon, Gerald Hartmann, A. Reiss, Brigitte Dietrich, Liu Yin, Ling Mingxing, and Guan Yili for elemental analyses. The constructive comments from Paul Tomascak, Joe Hiess and an anonymous reviewer and efficient editorial handling of Steven Shirey are greatly appreciated. This work was supported by the State Key Basic Research Development Program (Grant No. 2009CB825002), Academy of Science of China (No. KZCX2-YW-131), and the National Natural Science Foundation of China (Grant Nos. 40773013, 40921002).

APPENDIX A. SUPPLEMENTARY DATA

Supplementary data associated with this article can be found, in the online version, at doi:10.1016/j.gca.2011.04.011.

REFERENCES

Atherton M. P. and Petford N. (1993) Generation of sodium rich magmas from newly underplated basaltic crust. *Nature* **362**, 144–146.

Bea F., Pereira M. D. and Stroh A. (1994) Mineral/leucosome trace-element partitioning in a peraluminous migmatite (a laser ablation-ICP-MS study). *Chem. Geol.* **117**, 291–312.

Bedard J. H. (2006) Trace element partitioning in plagioclase feldspar. *Geochim. Cosmochim. Acta* **70**, 3717–3742.

Bindeman I. N. and Davis A. M. (2000) Trace element partitioning between plagioclase and melt: investigation of dopant influence on partition behavior. *Geochim. Cosmochim. Acta* **64**(16), 2863–2878.

Black L. P., Kamo S. L., Allen C. M., Aleinikoff J. K., Davis D. W., Korsch R. J. and Foudoulis C. (2003) TEMORA 1: a new zircon standard for Phanerozoic U–Pb geochronology. *Chem. Geol.* **200**, 155–170.

Blundy J. D. and Wood B. J. (1994) Prediction of crystal-melt partition coefficients from elastic moduli. *Nature* **372**, 452–453.

Brenan J. M., Shaw H. F., Ryerson F. J. and Phinney D. L. (1995) Experimental-determination of trace element partitioning between Pargasite and a synthetic hydrous andesitic melt. *Earth Planet. Sci. Lett.* **135**(1–4), 1–11.

Bryant D. L., Ayers J. C., Gao S., MIller C. F. and Zhang H. F. (2004) Geochemical, age, and isotopic constraints on the location of the Sino-Korean/Yangtze Suture and evolution of the Northern Dabie Complex, east central China. *Geol. Soc. Am. Bull.* **116**(5–6), 698–717.

Chappell B. W. and White A. J. R. (1992) I- and S-type granites in the Lachlan Fold Belt. *Trans. R. Soc. Edinburgh Earth Sci.* **83**, 1–26.

Chen B., Jahn B. M., Arakawa Y. and Zhai M. G. (2004) Petrogenesis of the Mesozoic intrusive complexes from the southern Taihang Orogen, North China Craton: elemental and Sr–Nd–Pb isotopic constraints. *Contrib. Mineral. Petrol.* **148**(4), 489–501.

Chen B., Jahn B. M. and Wei C. J. (2002) Petrogenesis of Mesozoic granitoids in the dabie UHP complex, central china: trace element and Nd–Sr isotope evidence. *Lithos* **60**(1–2), 67–88.

Chen B., Tian W., Jahn B. M. and Chen Z. C. (2008) Zircon SHRIMP U–Pb ages and in-situ Hf isotopic analysis for the Mesozoic intrusions in South Taihang, North China craton: evidence for hybridization between mantle-derived magmas and crustal components. *Lithos* **102**(1–2), 118–137.

Chung S. L., Liu D., Ji J., Chu M. F., Lee H. Y., Wen D. J., Lo C. H., Lee T. Y., Qian Q. and Zhang Q. (2003) Adakites from continental collision zones: melting of thickened lower crust beneath southern Tibet. *Geology* **31**(11), 1021–1024.

Compston W., Williams I. S., Kirschvink J. L., Zhang Z. C. and Ma G. (1992) Zircon U–Pb ages for the early Cambrian time-scale. *J. Geol. Soc. (London)* **149**, 171–184.

Condie K. C. (2005) TTGs and adakites: are they both slab melts? *Lithos* **80**(1–4), 33–44, special issue.

Defant M. J. and Drummond M. S. (1990) Derivation of some modern arc magmas by melting of young subducted lithosphere. *Nature* **347**(6294), 662–665.

Drake M. J. (1976) Plagioclase–melt equilibria. *Geochim. Cosmochim. Acta* **40**(4), 457–465.

Fan W. M., Guo F., Wang Y. J. and Zhang M. (2004) Late Mesozoic volcanism in the northern Huaiyang tectono-magmatic belt, central China: partial melts from a lithospheric mantle with subducted continental crust relicts beneath the Dabie orogen? *Chem. Geol.* **209**, 27–48.

Foley S. F., Barth M. G. and Jenner G. A. (2000) Rutile/melt partition coefficients for trace elements and assessment of the influence of rutile on the trace element characteristics of subduction zone magmas. *Geochim. Cosmochim. Acta* **64**.

Gao S., Ling W. L., Qiu Y. M., Lian Z., Hartmann G. and Simon K. (1999) Contrasting geochemical and Sm–Nd isotopic compositions of Archean metasediments from the Kongling high-grade terrain of the Yangtze craton: evidence for cratonic evolution and redistribution of REE during crustal anatexis. *Geochim. Cosmochim. Acta* **63**(13–14), 2071–2088.

Gao S., Luo T. C., Zhang B. R., Zhang H. F., Han Y. M., Zhao Z. D. and Hu Y. K. (1998) Chemical composition of the continental crust as revealed by studies in East China. *Geochim. Cosmochim. Acta* **62**(11), 1959–1975.

Gao S., Rudnick R. L., Yuan H. L., Liu X. M., Liu Y. S., Xu W. L., Ling W. L., Ayers J., Wang X. C. and Wang Q. H. (2004) Recycling lower continental crust in the North China craton. *Nature* **432**, 892–897.

Green T. H. (1994) Experimental studies of trace-element partitioning applicable to igneous petrogenesis–Sedona 16 years later. *Chem. Geol.* **117**, 1–36.

Guo F., Nakamuru E., Fan W. M., Kobayoshi K. and Li C. W. (2007) Generation of Palaeocene adakitic andesites by magma mixing; Yanji Area, NE China. *J. Petrol.* **48**(4), 661–692.

Hacker B. R., Ratschbacher L., Webb L., Ireland T., Walker D. and Dong S. W. (1998) U/Pb zircon ages constrain the architecture of the ultrahigh-pressure Oinling-Dabie Orogen, China. *Earth Planet. Sci. Lett.* **161**, 215–230.

Hou Z. H., Li S. G., Chen N. S., Li Q. L. and Liu X. M. (2005) Sm–Nd and zircon SHRIMP U–Pb dating of Huilanshan mafic granulite in the Dabie Mountains and its zircon trace element geochemistry. *Sci. China (Ser. D)* **48**(12), 2081–2091.

Huang F. and He Y. S. (2010) Partial melting of the dry mafic continental crust and C-type adakites. *Chin. Sci. Bull.* **55**(13), 1255–1267.

Huang F., Li S. G., Dong F., He Y. S. and Chen F. K. (2008) High-Mg adakitic rocks in the Dabie orogen, central China: implications for foundering mechanism of lower continental crust. *Chem. Geol.* **255**(1–2), 1–13.

Huang F., Li S. G., Dong F., Li Q. L., Chen F. K., Wang Y. and Yang W. (2007) Recycling of deeply subducted continental crust in the Dabie Mountains, central China. *Lithos* **96**, 151–169.

Huang F., Lundstrom C. C. and McDonough W. F. (2006) Effect of melt structure on trace-element partitioning between clinopyroxene and silicic, alkaline, aluminous melts. *Am. Mineral.* **91**, 1385–1400.

Irvine T. N. and Baragar W. R. (1971) A guide to the chemical classification of the common volcanic rocks. *Can. J. Earth Sci.* **8**, 523–548.

Jahn B. M., Wu F. Y., Lo C. H. and Tsai C. H. (1999) Crust-mantle interaction induced by deep subduction of the continental crust: geochemical and Sr–Nd isotopic evidence from post-collisional mafic-ultramafic intrusions of the northern Dabie complex, central China. *Chem. Geol.* **157**, 119–146.

Jiang N., Liu Y. S., Zhou W. G., Yang J. H. and Zhang S. Q. (2007) Derivation of Mesozoic adakitic magmas from ancient lower crust in the North China craton. *Geochim. Cosmochim. Acta* **71**(10), 2591–2608.

Kamei A., Miyake Y., Owada M. and Kimura J. I. (2009) A pseudo adakite derived from partial melting of tonalitic to granodioritic crust, Kyushu, southwest Japan arc. *Lithos* **112**, 615–625.

Kay R. W. and Kay S. M. (1993) Delamination and delamination magmatism. *Tectonophysics* **219**(1–3), 177–189.

Klein M., Stosch H. G., Seck H. A. and Shimizu N. (2000) Experimental partitioning of high field strength and rare earth elements between clinopyroxene and garnet in andesitic to tonalitic systems. *Geochim. Cosmochim. Acta* **64**(1), 99–115.

Klemme S., Prowatke S., Hametner K. and Gunther D. (2005) Partitioning of trace elements between rutile and silicate melts: Implications for subduction zones. *Geochim. Cosmochim. Acta* **69**(9), 2361–2371.

Li J. W., Zhao X. F., Zhou M. F., Ma C. Q., de Souza Z. S. and Vasconcelos P. (2009) Late Mesozoic magmatism from the Daye region, eastern China: U–Pb ages, petrogenesis, and geodynamic implications. *Contrib. Mineral. Petrol.* **157**(3), 383–409.

Liu S.-A., Li S. G., He Y. S. and Huang F. (2010a) Geochemical contrasts between early Cretaceous ore-bearing and ore-barren high-Mg adakites in central-eastern China: implications for petrogenesis and Cu–Au mineralization. *Geochim. Cosmochim. Acta* **74**(24), 7160–7178.

Liu S. A., Teng F. Z., Li S. G., He Y. S. and Ke S. (2010b) Investigation of magnesium isotope fractionation during granite differentiation: implication for Mg isotopic composition of the continental crust. *Earth Planet. Sci. Lett.* **297**(3–4), 646–654.

Li S. G., Jagoutz E., Chen Y. Z. and Li Q. L. (2000) Sm–Nd and Rb–Sr isotopic chronology and cooling history of ultrahigh pressure metamorphic rocks and their country rocks at Shuanghe in the Dabie Mountains, Central China. *Geochim. Cosmochim. Acta* **64**(6), 1077–1093.

Li S. G., Hong J. A., Li H. M. and Jiang L. L. (1999) Zircon U–Pb datings of pyroxenite–gabbro intrusions in the Dabie orogen and their geological implications. *Geol. J. Chinese Univ.* **5**(3), 351–355 (in Chinese with English abstract).

Li S. G., Huang F., Nie Y. H., Han W. L., Long G., Li H. M., Zhang S. Q. and Zhang Z. H. (2001) Geochemical and geochronological constraints on the suture location between the North and South China Blocks in the Dabie orogen, central China. *Phys. Chem. Earth (A)* **26**(9–10), 655–672.

Li S. G., Nie Y. H., Zheng S. G. and Liu D. L. (1998a) Interaction between subducted continental crust and the mantle. I: Major and trace element geochemistry of the syncollisional mafic–altrumafic intrusions in the Dabie Mountains. *Sci. China (Ser. D)* **41**(5), 545–552.

Li S. G., Nie Y. H., Hart S. R. and Zhang Z. Q. (1998b) Interaction between subduted continental crust and the mantle. II: Sr and Nd isotopic geochemistry of the syncollisional mafic–ultramafic intrusions in the Dabie Moutains. *Sci. China (Ser. D)* **41**(6), 632–638.

Li S. G., Xiao Y. L., Liou D. L., Chen Y. Z., Ge N. J., Zhang Z. Q., Sun S. S., Cong B. L., Zhang R. Y., Hart S. R. and Wang S. S. (1993) Collision of the North China and Yangtse Blocks and Formation of Coesite-Bearing Eclogites – Timing and Processes. *Chem. Geol.* **109**(1–4), 89–111.

Liu D. Y., Jian P., Kroener A. and Xu S. T. (2006) Dating of prograde metamorphic events deciphered from episodic zircon growth in rocks of the Dabie-Sulu UHP complex, China. *Earth Planet. Sci. Lett.* **250**, 650–666.

Liu Y., Liu X. M., Hu Z. C., Diwu C. R., Yuan H. L. and Gao S. (2007a) Evaluation of accuracy and long-term stability of determination of 37 trace elements in geological samples by ICP-MS. *Acta Petrol. Sinica* **23**(5), 1203–1210.

Liu Y. C., Li S. G. and Xu S. T. (2007b) Zircon SHRIMP U–Pb dating for gneisses in northern Dabie high TIP metamorphic zone, central China: implications for decoupling within subducted continental crust. *Lithos* **96**(1–2), 170–185.

Ludwig, K. R. (2001) Users manual for isoplot/Ex (rev.2.4.9): a geochronological toolkit for microsoft excel. Berkeley Geochronol. Center. Special Publication, No. 1a, p. 55.

Ma C. Q., Ehlers C., Xu C. H., Li Z. C. and Yang K. G. (2000) The roots of the Dabieshan ultrahigh-pressure metamorphic terrane: constraints from geochemistry and Nd–Sr isotope systematics. *Precambrian Res.* **102**, 279–301.

Ma C. Q., Li Z. C., Ehlers C., Yang K. G. and Wang R. J. (1998) A post-collisional magmatic plumbing system: mesozoic granitoid plutons from the Dabieshan high-pressure and ultrahigh-pressure metamorphic zone, east-central China. *Lithos* **45**, 431–456.

Ma C. Q., Yang K. G., Ming H. L. and Lin G. C. (2003) The age of transformation for the Mesozoic crust of the Dabie orogen from compression to extension: evidences from granites. *Sci. China (Ser. D)* **33**(9), 817–827.

Macpherson C. G., Dreher S. T. and Thirlwall M. F. (2006) Adakites without slab melting: high pressure differentiation of island arc magma, Mindanao, the Philippines. *Earth Planet. Sci. Lett.* **243**(3–4), 581–593.

Martin H. (1999) Adakitic magmas: modern analogues of Archaean granitoids. *Lithos* **46**(3), 411–429.

Martin H., Smithies R. H., Rapp R., Moyen J. F. and Champion D. (2005) An overview of adakite, tonalite–trondhjemiten–granodiorite (TTG), and sanukitoid: relationships and some implications for crustal evolution. *Lithos* **79**(1–2), 1–24, special issue.

Middlemost E. A. K. (1985) Naming materials in the magma/igneous rock system. *Earth Sci. Rev.* **37**, 215–224.

Mo X. X., Hou Z. Q., Niu Y. L., Dong G. C., Qu X. M., Zhao Z. D. and Yang Z. M. (2007) Mantle contributions to crustal thickening during continental collision: evidence from Cenozoic igneous rocks in southern Tibet. *Lithos* **96**(1–2), 225–242.

Moyen J. F. (2009) High Sr/Y and La/Yb ratios: the meaning of the 'adakitic signature'. *Lithos* **112**, 556–574.

Moyen, J. F. and Stevens, G. (2006) Experimental constraints on TTG petrogenesis: implications for Archean geodynamics. In: *Archean Geodynamics and Environments, Monographs* (eds. K. Benn, J.-C. Mareschal, K.C. Condie). AGU. pp. 149–178.

Nash W. P. and Crecraft H. R. (1985) Partition coefficients for trace elements in silicic magmas. *Geochim. Cosmochim. Acta* **49**(2), 309–322.

Okay A. I., Xu S. T. and Sengor A. M. C. (1989) Coesite from the Dabie Shan Eclogites, Central China. *Eur. J. Mineral.* **1**(4), 595–598.

Patino Douce A. E. (2005) Vapor-absent melting of tonalite at 15–32 kbar. *J. Petrol.* **46**(2), 275–290.

Prowatke S. and Klemme S. (2005) Effect of melt composition on the partitioning of trace elements between titanite and silicate melt. *Geochim. Cosmochim. Acta* **69**(3), 695–709.

Pertermann, M., Hirschmann, M. M., Hametner, K., Gunther, D. and Schmidt, M. W. (2004) Experimental determination of trace element partitioning between garnet and silica-rich liquid during anhydrous partial melting of MORB-like eclogite. *Geochem. Geophys. Geosyst.* 5(Q05A01). doi:10.1029/2003GC000638.

Qian C. C., Lu Y. L. and Liu L. L. (2004) Geochemical characteristics and genesis of Yanshanian granite in the Dabie ultrahigh-pressure (UHP) metamorphic belt. *Geol. China* **31**(2), 147–154.

Rapp R. (1995) Amphibole-out phase boundary in partially melted metabasalt, its control over liquid fraction and composition, and source permeability. *J. Geophys. Res.* **100**, 15601–15610.

Rapp R. and Watson E. B. (1995) Dehydration melting of metabasalt at 8–32 kbar: implications for continental growth and crust-mantle recycling. *J. Petrol.* **36**, 891–931.

Rapp, R., Watson, E. B. and MIller, C. F. (1991) Partial melting of amphibolite/eclogite and the origin of Archean trondhjemites and tonalities. *Precambrian Res.* 51.

Rapp R. P., Shimizu N., Norman M. D. and Applegate G. S. (1999) Reaction between slab-derived melts and peridotite in the mantle wedge: experimental constraints at 3.8 GPa. *Chem. Geol.* **160**(4), 335–356.

Richards J. R. and Kerrich R. (2007) Special paper: Adakite-like rocks: their diverse origins and questionable role in metallogenesis. *Econ. Geol.* **102**, 537–576.

Rudnick R. L. and Gao S. (2003) Composition of the continental crust. In the Crust (ed. R.L. Rudnick), 3 Treatise on Geochemistry (eds. H.D. Holland and K.K. Turekian), Elsevier-Pergamon, Oxford. pp. 1–64.

Sen C. and Dunn T. (1994) Dehydration melting of a basaltic composition amphibolite at 1.5 and 2.0 GPa: implications for the origin of adakites. *Contrib. Mineral. Petrol.* **117**(4), 394–409.

Shaw D. M. (1970) Trace element fractionation during anatexis. *Geochim. Cosmochim. Acta* **34**(2), 237–243.

Skjerlie K. P. and Johnston A. D. (1996) Vapour-absent melting from 10 to 20 kbar of crustal rocks that contain multiple hydrous phases: implications for anatexis in the deep to very deep continental crust and active continental margins. *J. Petrol.* **37**(3), 661–691.

Smithies R. H. (2000) The Archaean tonalite–trondhjemite–granodiorite (TTG) series is not an analogue of Cenozoic adakite. *Earth Planet. Sci. Lett.* **182**(1), 115–125.

Steiger R. H. and Jäger E. (1977) Subcommision on geochronology: convention on the use of decay constants in Geo- and cosmochronology. *Earth Planet. Sci. Lett.* **36**, 359–362.

Sun S. S. and McDonough W. F. (1989) Chemical and isotopic systematics of oceanic basalts: implication for mantle composition and process. In: *Magmatism in the Ocean Basins* (eds. A.D. Saunders, M.J. Norry), 42, pp. 313–345.

Tang J., Zheng Y. F., Wu Y. B., Gong B., Zha X. P. and Liu X. M. (2008) Zircon U–Pb age and geochemical contraints on the tectonic affinity of the Jiaodong terrane in the Sulu orogen, China. *Precambrian Res.* **161**, 389–418.

Wang J. H. and Deng S. X. (2002) Emplacement age for the mafic–ultramafic plutons in the northern Dabie Mts. (Hubei): Zircon U–Pb, Sm–Nd and $^{40}Ar/^{39}Ar$ dating. *Sci. China (Ser. D)* **45**(1), 1–12.

Wang Q., McDermott F., Xu J. F., Bellon H. and Zhu Y. T. (2005) Cenozoic K-rich adakitic volcanic rocks in the Hohxil area, northern Tibet: lower-crustal melting in an intracontinental setting. *Geology* **33**(6), 465–468.

Wang Q., Wyman D. A., Xu J. F., Jian P., Zhao Z. H., Li C. F., Xu W., Ma J. L. and He B. (2007a) Early Cretaceous adakitic granites in the Northern Dabie Complex, central China: implications for partial melting and delamination of thickened lower crust. *Geochim. Cosmochim. Acta* **71**(10), 2609–2636.

Wang Q., Wyman D. A., Xu J. F., Zhao Z. H., Jian P., Xiong X. L., Bao Z. W., Li C. F. and Bai Z. H. (2006) Petrogenesis of Cretaceous adakitic and shoshonitic igneous rocks in the Luzong area, Anhui Province (eastern China): implications for geodynamics and Cu–Au mineralization. *Lithos* **89**(3–4), 424–446.

Wang Q., Wyman D. A., Xu J. F., Zhao Z. H., Jian P. and Zi F. (2007b) Partial melting of thickened or delaminated lower crust in the middle of eastern China: implications for Cu–Au mineralization. *J. Geol.* **115**(2), 149–161.

Wang Q., Xu J. F., Zhao Z. H., Bao Z. W., Xu W. and Xiong X. L. (2004a) Cretaceous high-potassium intrusive rocks in the Yueshan–Hongzhen area of east China: adakites in an extensional tectonic regime within a continent. *Geochem. J.* **38**(5), 417–434.

Wang Q., Zhao Z. H., Bao Z. W., Xu J. F., Liu W., Li C. F., Bai Z. H. and Xiong X. L. (2004b) Geochemistry and petrogenesis of the Tongshankou and Yinzu adakitic intrusive rocks and the associated porphyry copper–molybdenum mineralization in southeast Hubei, east China. *Resour. Geol.* **54**(2), 137–152.

Wang X., Liou J. G. and Mao H. J. (1989) Coesite-bearing eclogites from the Dabie Mountains in central China. *Geology* **17**, 1085–1088.

Watkins J. M., Clemens J. D. and Treloar P. J. (2007) Archean TTGs as sources of younger granitic magmas: melting of sodic metatonalites at 0.6–1.2 GPa. *Contrib. Mineral. Petrol.* **154**, 91–110.

Weaver B. L. and Tarney J. (1984) Empirical approach to estimating the composition of the continental crust. *Nature* **310**, 575–577.

Williams I. S. (1998) U–Th–Pb geochronology by ion microprobe. *Rev. Econ. Geol.* **7**, 1–35.

Xia Q.-X., Zheng Y.-F. and Zhou L.-G. (2008) Dehydration and melting during continental collision: constraints from element and isotope geochemistry of low-T/UHP granitic gneiss in the Dabie orogen. *Chem. Geol.* **247**(1–2), 36–65.

Xie Z., Zheng Y. F., Yan J. and Qian H. (2004) Source evolution relationship between A-type granites and mafic rocks from Shacun in Dabieshan. *Acta Petrol. Sinica* **20**(5), 1175–1184.

Xie Z., Zheng Y. F., Zhao Z. F., Wu Y. B., Wang Z. R., Chen J. F., Liu X. M. and Wu F. Y. (2006) Mineral isotope evidence for the contemporaneous process of Mesozoic granite emplacement and gneiss metamorphism in the Dabie orogen. *Chem. Geol.* **231**, 214–235.

Xiong X. L., Adam J. and Green T. H. (2005) Rutile stability and rutile/melt HFSE partitioning during partial melting of hydrous basalt: implications for TTG genesis. Chem. Geol. 218.

Xu H. J., Ma C. Q. and Ye K. (2007) Early cretaceous granitoids and their implications for the collapse of the Dabie orogen, eastern China: SHRIMP zircon U–Pb dating and geochemistry. *Chem. Geol.* **240**(3–4), 238–259.

Xu H. J., Ye K. and Ma C. Q. (2008) Early Cretaceous granitoids in the North Dabie and their tectonic implications: Sr–Nd and zircon Hf isotopic evidences. *Acta Petrol. Sinica* **24**(1), 87–103.

Xu J. F., Shinjo R., Defant M. J., Wang Q. and Rapp R. P. (2002) Origin of Mesozoic adakitic intrusive rocks in the Ningzhen area of east China: partial melting of delaminated lower continental crust? *Geology* **30**(12), 1111–1114.

Xu S. T., Okay A. I., Ji S. Y., Sengor A. M. C., Wen S., Liu Y. C. and Jiang L. L. (1992) Diamond from the Dabie-Shan metamorphic rocks and its implication for tectonic setting. *Science* **256**(5053), 80–82.

Xu X. J., Zhao Z. F., Zheng Y. F. and Wei C. S. (2005) Element and isotope geochemistry of Mesozoic intermediate-felsic rocks at Tianzhushan in the Dabie orogen. *Acta Petrol. Sinica* **21**(3), 607–622.

Ye K., Yao Y. P., Katayama I., Cong B. L., Wang Q. C. and Maruyama S. (2000) Large areal extent of ultrahigh-pressure metamorphism in the Sulu ultrahigh-pressure terrane of East China: new implications from coesite and omphacite inclusions in zircon of granitic gneiss. *Lithos* **52**(1–4), 157–164.

Yuan X. C., Klemperer S. L., Teng W. B., Liu L. X. and Chetwin E. (2003) Crustal structure and exhumation of the Dabie shan ultrahigh-pressure orogen, eastern China, from seismic reflection profiling. *Geology* **31**(5), 435–438.

Zhang H. F., Gao S., Zhong Z. Q., Zhang B. R., Zhang L. and Hu S. H. (2002) Geochemical and Sr–Nd–Pb isotopic compositions of Cretaceous granitoids: constraints on tectonic framework and crustal structure of the Dabieshan ultrahigh-pressure metamorphic belt, China. *Chem. Geol.* **186**, 281–299.

Zhang C., Ma C. Q. and Holtz F. (2010) Origin of high-Mg adakitic magmatic enclaves from the Meichuan pluton, southern Dabie orogen (central China): Implications for delamination of the lower continental crust and melt-mantle interaction. *Lithos* **119**, 467–484.

Zhang Q., Wang Y., Qian Q., Yang J. H., Wang Y. L., Zhao T. P. and Guo G. J. (2001) The characteristics and tectonic–metallogenic significances of the adakites in Yanshan period from eastern China. *Acta Petrol. Sinica* **17**(02), 236–244.

Zhang S. B., Zheng Y. F., Wu Y. B., Zhao Z. F., Gao S. and Wu F. Y. (2006) Zircon U–Pb age and Hf–O isotope evidence for Paleoproterozoic metamorphic event in South China. *Precambrian Res.* **151**, 265–288.

Zhang S. B., Zheng Y. F., Zhao Z. F., Wu Y. B., Yuan H. L. and Wu F. Y. (2009) Origin of TTG-like rocks from anatexis of ancient lower crust: geochemical evidence from neoproterozoic granitoids in South China. *Lithos* **113**, 347–368.

Zhao X. F., Li J. W., Ma C. Q. and Lang Y. S. (2007a) Geohronology and geochemistry of the Gubei granodiorite, north Huaiyang: implications for Mesozoic tectonic transition of the Dabie orogen. *Acta Petrol. Sinica* **23**(6), 1392–1402.

Zhao Z. F., Zheng Y. F., Chen R. X., Xia Q. X. and Wu Y. B. (2007b) Element mobility in mafic and felsic ultrahigh-pressure metamorphic rocks during continental collision. *Geochim. Cosmochim. Acta* **71**, 5244–5266.

Zhao Z. F., Zheng Y. F., Wei C. S. and Wu Y. B. (2004) Zircon U–Pb age, element and oxygen isotope geochemistry of Mesozoic intermediate-felsic rocks in the Dabie Mountains. *Acta Petrol. Sinica* **20**(5), 1151–1174.

Zhao Z. F., Zheng Y. F., Wei C. S. and Wu Y. B. (2007c) Post-collisional granitoids from the Dabie orogen in China: Zircon U–Pb age, element and O isotope evidence for recycling of subducted continental crust. *Lithos* **93**, 248–272.

Zhao Z. F., Zheng Y. F., Wei C. S., Wu Y. B., Chen F. K. and Jahn B. M. (2005) Zircon U–Pb age, element and C–O isotope geochemistry of post-collisional mafic–ultramafic rocks from the Dabie orogen in east-central China. *Lithos* **83**, 1–28.

Zhao Z. F. and Zheng Y. F. (2009) Remelting of subducted continental lithosphere: Petrogenesis of Mesozoic magmatic rocks in the Dabie-Sulu orogenic belt. *Sci. China Ser. D. Earth Sci.* **2009**, 52. doi:10.1007/s11430-009-0134-8.

Zheng Y. F., Fu B., Gong B. and Li L. (2003) Stable isotope geochemistry of ultrahigh pressure metamorphic rocks from the Dabie-Sulu orogen in China: implications for geodynamics and fluid regime. *Earth Sci. Rev.* **62**(1–2), 105–161.

Associate editor: Steven B. Shirey